Lecture #20 Hot Topics: ^{13}C MRS

- Neurotransmission
- ^{13}C MRS
- Hyperpolarized ^{13}C MRS
- References
  - Rothman, et al., "^{13}C MRS studies of neuroenergetics and neurotransmitter cycling in humans", NMR Biomedicine, 2011 Oct; 24(8):943-57.
  - Hurd et al., "Hyperpolarized ^{13}C Metabolic Imaging Using Dissolution Dynamic Nuclear Polarization", JMR 36:1314–1328 (2012) .

Neurons and Neurotransmission

- Neurons carry action potentials, but are not directly connected.
- Axon-dendrite connections rely on chemicals (neurotransmitters).
- Neurotransmitters can be excitatory or inhibitory.

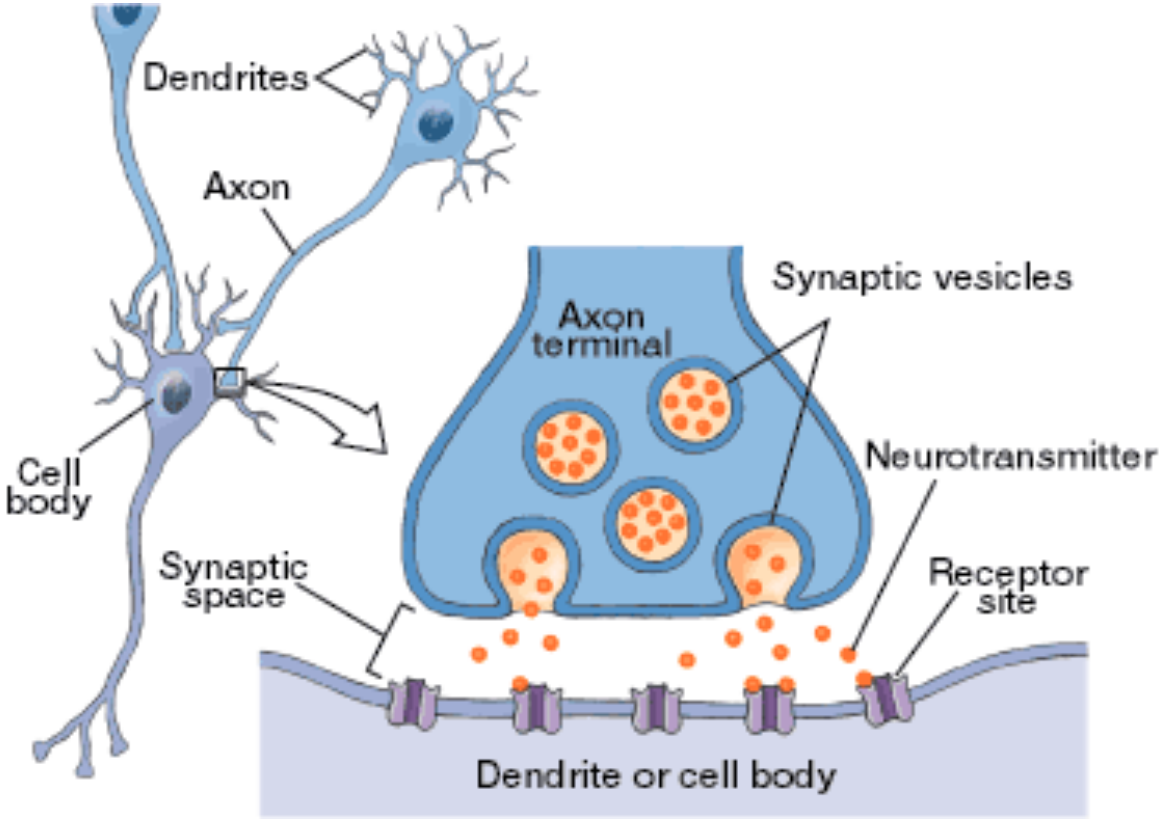

Glutamate is the major excitatory neurotransmitter in the human brain with >80% of synapses utilizing glutamate.

Thomas C. Südhof
Stanford University

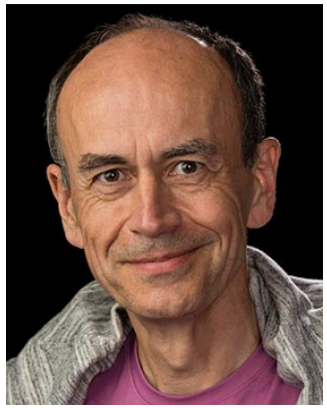

The Nobel Prize in Physiology or Medicine 2013

The brain in more than just neurons..

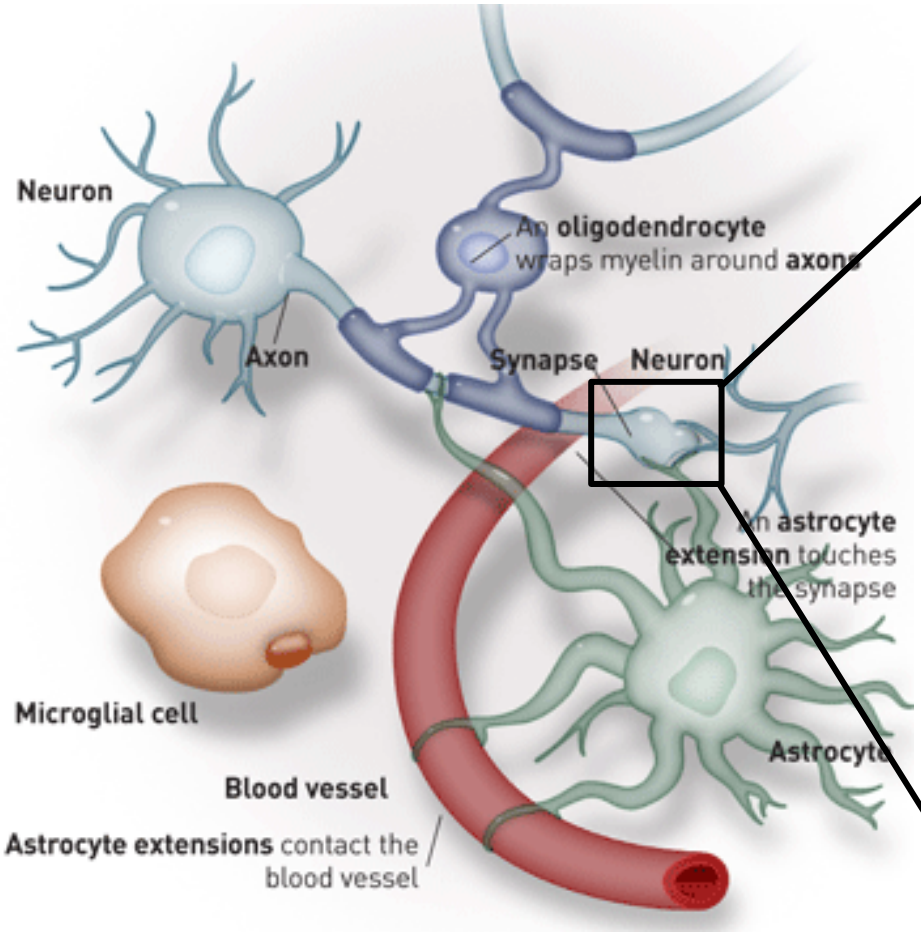

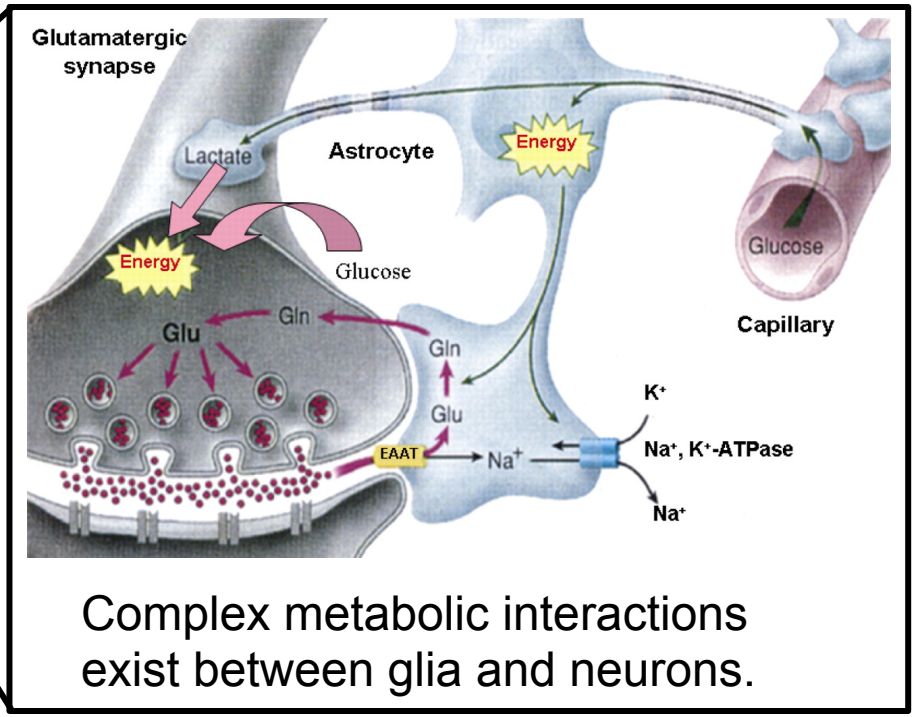

Complex metabolic interactions exist between glia and neurons.

Energy metabolism is coupled with neurotransmission.

Neurotransmitter Cycling

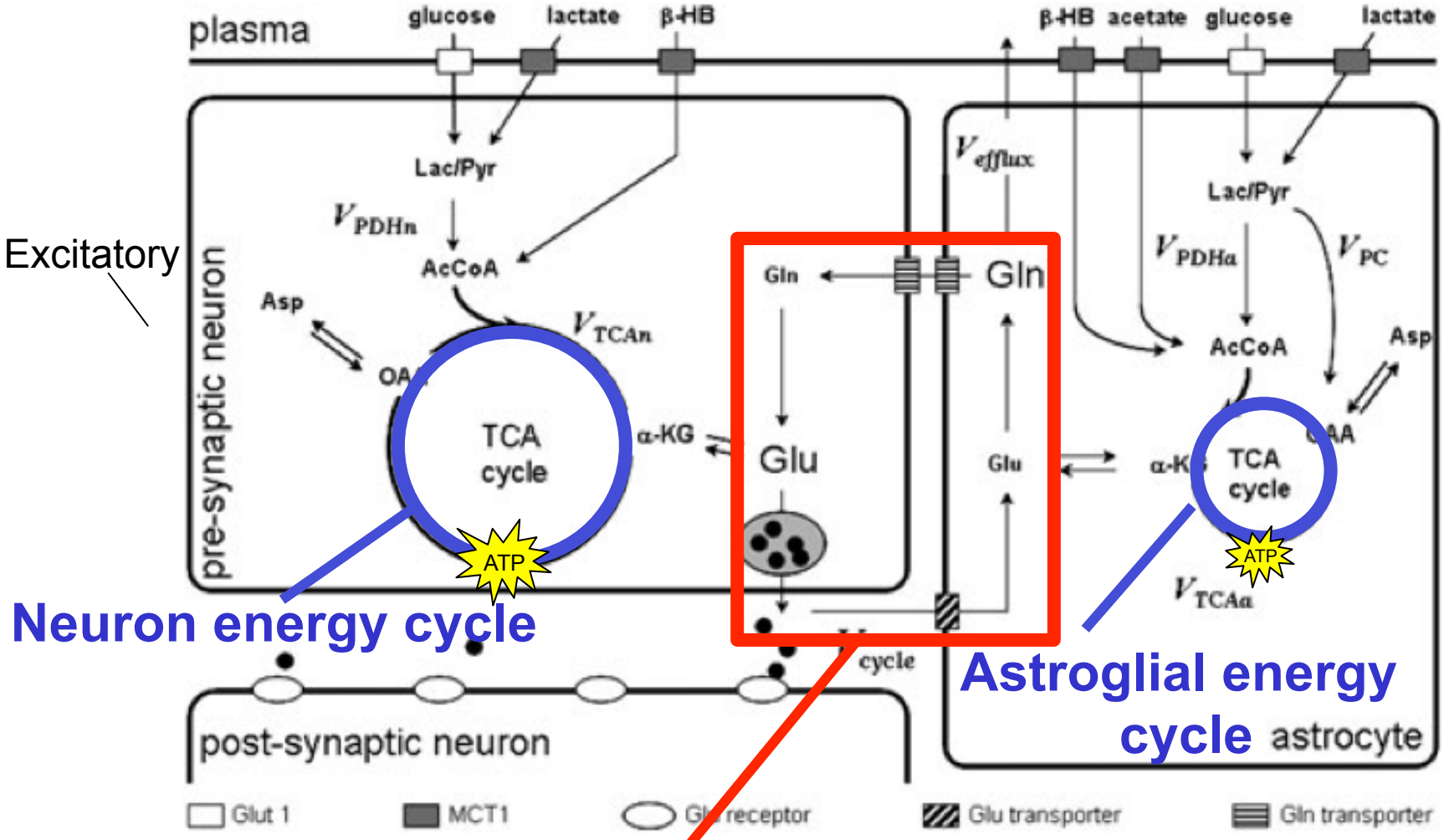

Excitatory

Neuron energy cycle

Astroglial energy cycle

Glutamate-Glutamine cycle

Rothman, et al, NMR Biomedicine, 2011.

Probing Brain Function with Carbon

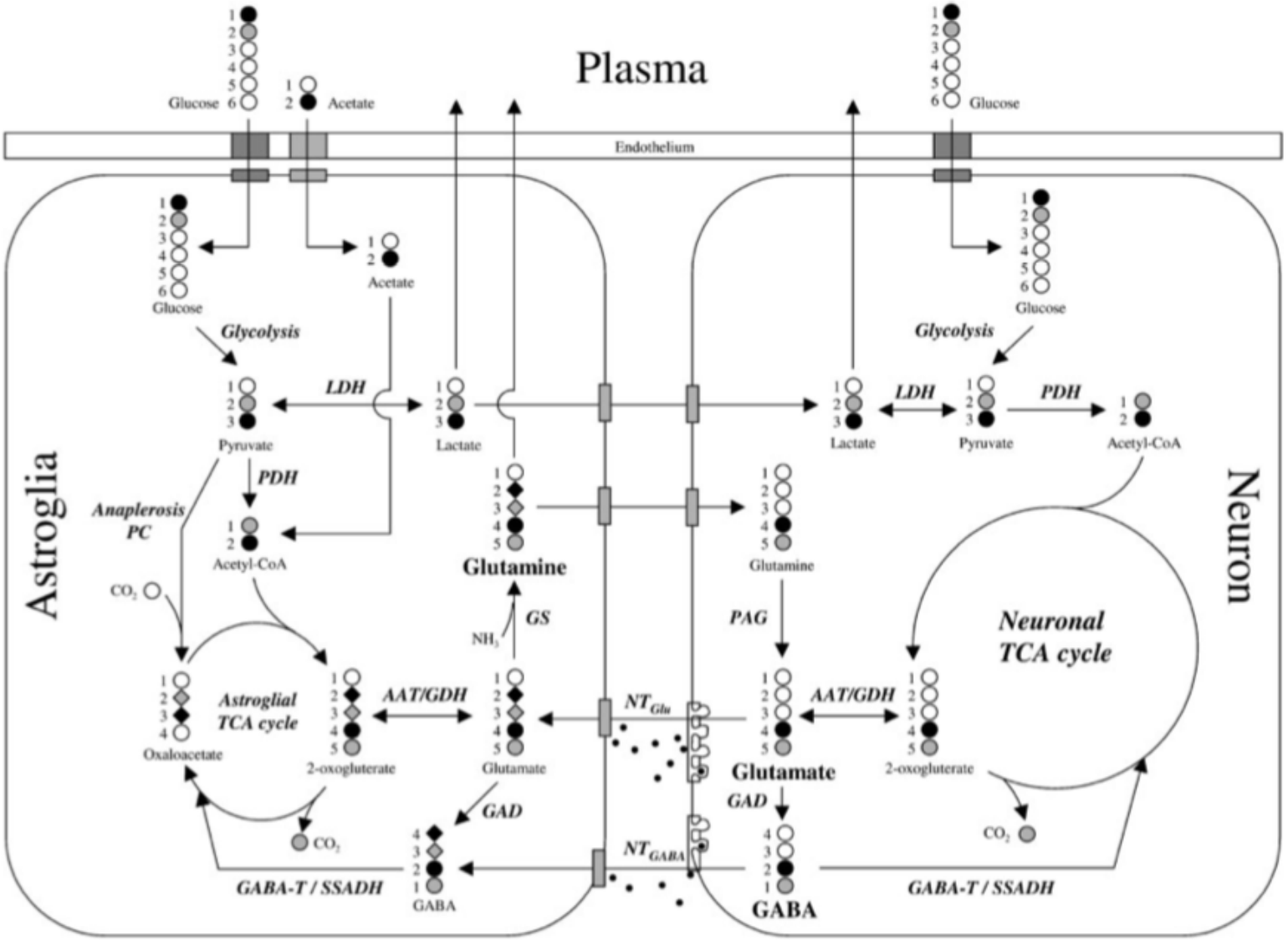

de Graaf, et al, NMR Biomedicine, 2003.

Probing Brain Function with ^{13}C MRS

Collect spectra

Infuse ^{13}C-glucose
(or ^{13}C-acetate)

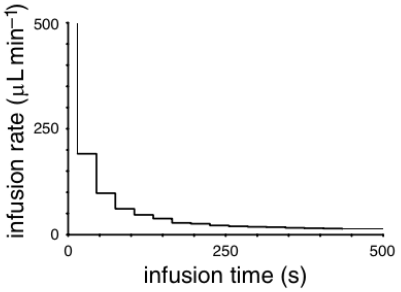

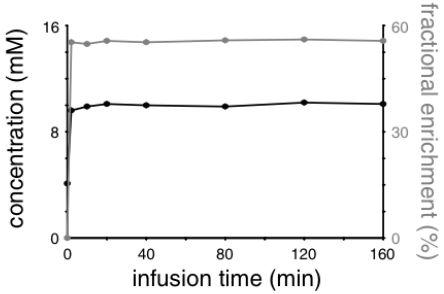

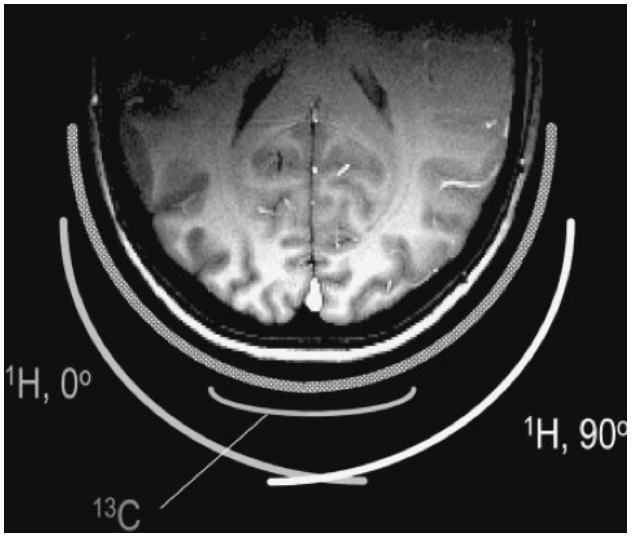

Quantify spectra
over time

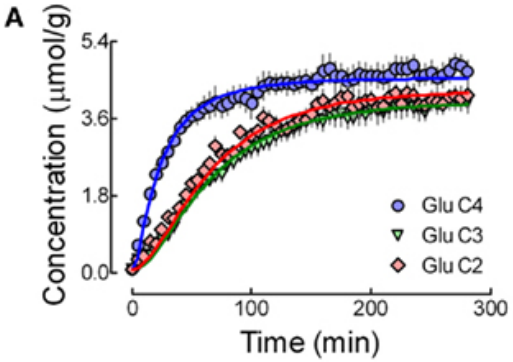

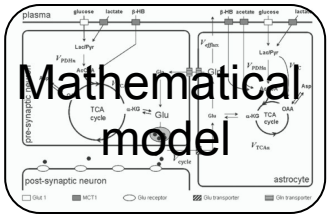

Mathematical model

V_{TCAn} = neuron TCA flux

V_{TCAg} = glial TCA flux

V_{NT} = Glu/Gln neurotransmitter flux

Metabolic Modeling

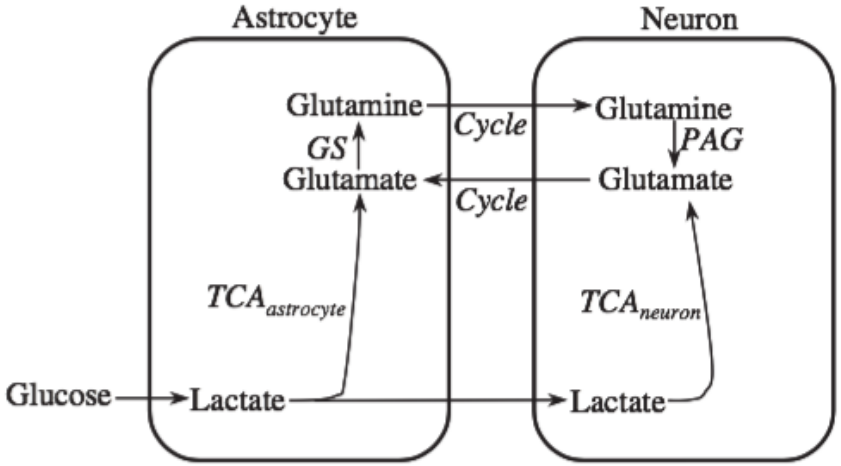

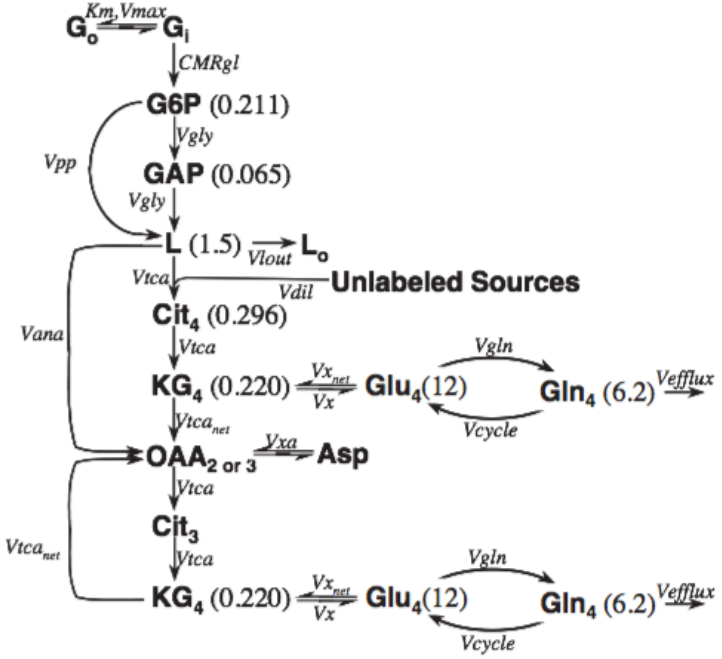

$$\frac{d\mathrm{Glu}_4}{dt} = \frac{L_3}{L}\mathrm{Vgly} + \frac{\mathrm{Gln}_4}{\mathrm{Gln}}\mathrm{Vcycle} + (0)\mathrm{Vdil} - \frac{\mathrm{Glu}_4}{\mathrm{Gln}}(\mathrm{Vtca} + \mathrm{Vgln}),$$

$$\frac{d\mathrm{Gln}_4}{dt} = \frac{\mathrm{Glu}_4}{\mathrm{Glu}}\mathrm{Vgln} - \frac{\mathrm{Gln}_4}{\mathrm{Gln}}(\mathrm{Vcycle} + \mathrm{Vefflux}),$$

$$\frac{d\mathrm{Glu}_3}{dt} = \frac{1}{2}\frac{L_3}{L}\mathrm{Vana} + \frac{1}{2}(0)\mathrm{Vana} + \frac{1\mathrm{Glu}_4}{2\,\mathrm{Glu}}\mathrm{Vtca}_{\mathrm{net}} + \frac{1\mathrm{Glu}_3}{2\,\mathrm{Glu}}\mathrm{Vtca}_{\mathrm{net}} + \frac{\mathrm{Gln}_3}{\mathrm{Gln}}\mathrm{Vcycle} - \frac{\mathrm{Glu}_3}{\mathrm{Glu}}(\mathrm{Vtca} + \mathrm{Vgln}),$$

$$\frac{d\mathrm{Gln}_3}{dt} = \frac{\mathrm{Glu}_3}{\mathrm{Glu}}\mathrm{Vgln} - \frac{\mathrm{Gln}_3}{\mathrm{Gln}}(\mathrm{Vcycle} + \mathrm{Vefflux}),$$

$$\frac{d\mathrm{Glu}_{3,4}}{dt} = \frac{L_3}{L}\frac{\mathrm{Glu}_3}{\mathrm{Glu}}\mathrm{Vtca} + \frac{\mathrm{Gln}_{3,4}}{\mathrm{Gln}}\mathrm{Vcycle} - \frac{\mathrm{Glu}_{3,4}}{\mathrm{Glu}}(\mathrm{Vtca} + \mathrm{Vgln}),$$

$$\frac{d\mathrm{Gln}_{3,4}}{dt} = \frac{\mathrm{Glu}_{3,4}}{\mathrm{Glu}}\mathrm{Vgln} - \frac{\mathrm{Gln}_{3,4}}{\mathrm{Gln}}(\mathrm{Vcycle} + \mathrm{Vefflux}).$$

$^{N}V_{TCA}$, rate of neuronal TCA cycle
$^{A}V_{TCA}$, rat of astroglial TCA cycle
V_{cycle}, rate of Glu-Gln cycle;

Mason, et al., Metabolic Engineering 6, 75-84, 2004

Probing Brain Function with ^{13}C MRS

Glutamate

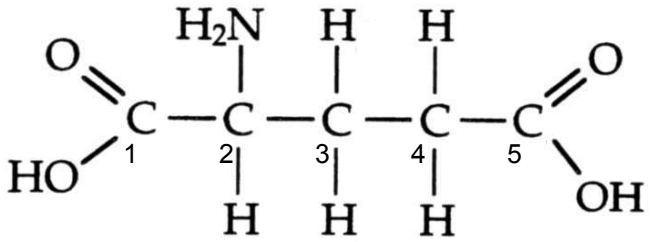

Glutamine

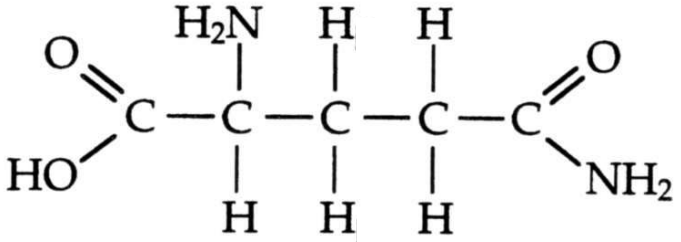

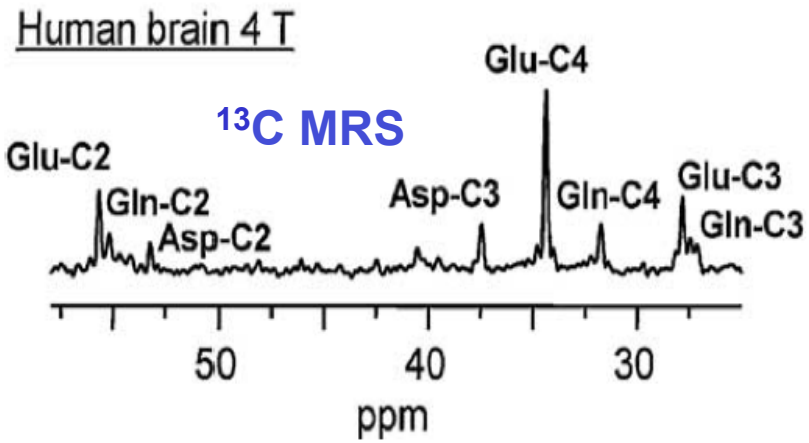

~45 cc, 10 min acq

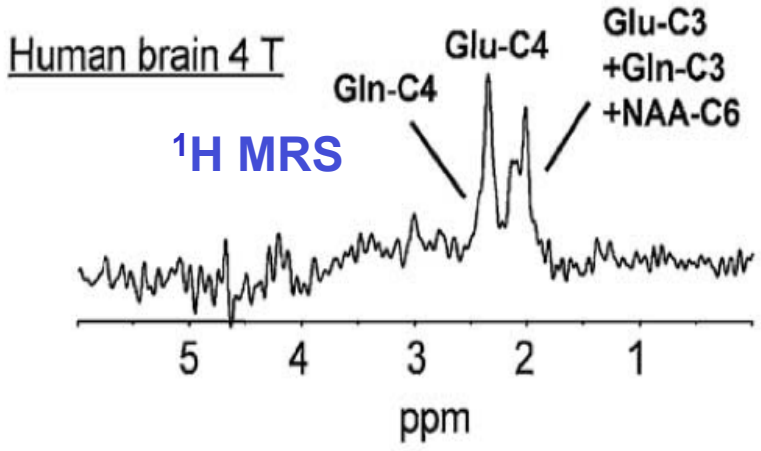

~10 cc, 10 min acq

^{13}C and ^{1}H spectra from human visual cortex during an infusion of [1-^{13}C]glucose.

Hardware

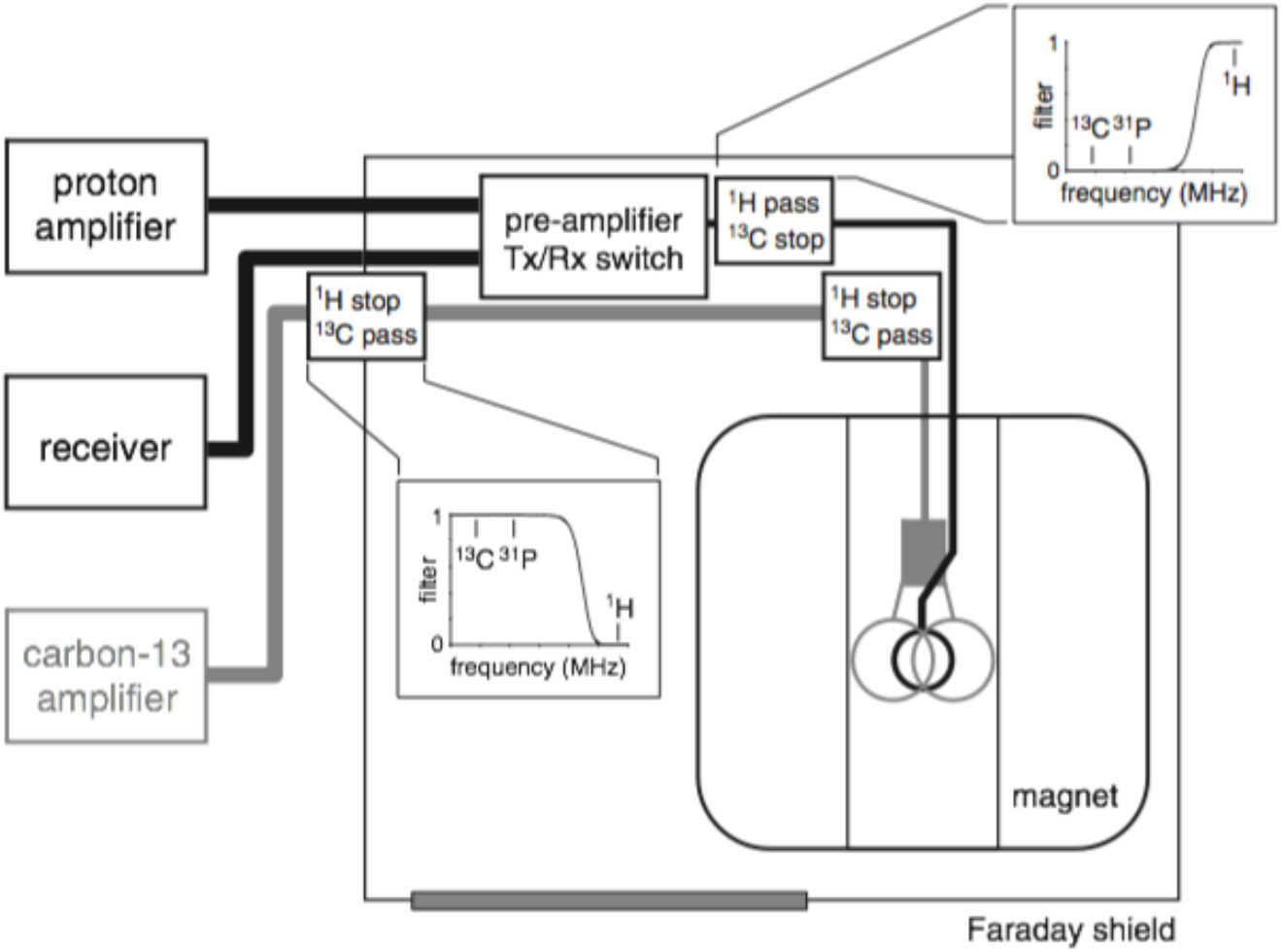

de Graaf, et al, NMR Biomed 2011

Multinuclear Pulse Sequences

Direct Detection

For in vivo ^{13}C-infusion brain studies (e.g. labeled glucose or acetate) …

- ^{13}C spectrum: low sensitivity, excellent peak discrimination.
- Simple ^{13}C excitation and detection is rarely used do to poor sensitivity
- Polarization transfer is commonly used: INEPT, DEPT
- Almost all methods use decoupling.

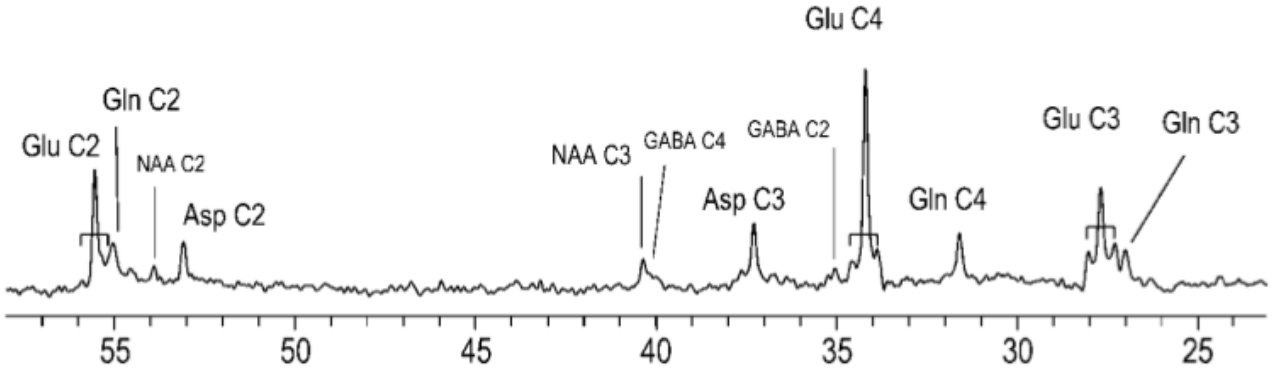

4T ^{13}C spectrum obtained from a 45 ml volume in the human visual cortex during an infusion of 67%-enriched [1-^{13}C]glucose. (DEPT sequence).

Gruetter, et al., NMR Biomed 2003.

Polarization Transfer

- MRI sensitivity given by

$$SNR \propto \frac{\left(\frac{\gamma\hbar B_0}{2kT}\right)\left(\frac{\gamma\hbar}{2}\right)\left(\gamma B_0\right)}{\gamma B_0} = \frac{\gamma^2\hbar^2 B_0}{4kT}$$

polarization; magnetic moment; ω_0; noise

- In polarization transfer, we seek to exploit ^{1}H-^{13}C J coupling to find a pulse sequence with sensitivity given by…

$$SNR \propto \frac{\left(\frac{\gamma_H\hbar B_0}{2kT}\right)\left(\frac{\gamma_C\hbar}{2}\right)\left(\gamma_C B_0\right)}{\gamma_C B_0} = \frac{\gamma_H\gamma_C\hbar^2 B_0}{4kT}$$

"proton" polarization; "carbon" detecton

- Given $\gamma_H \approx 4\gamma_C$, this will yield a 4x sensitivity increase!

Methods: INEPT

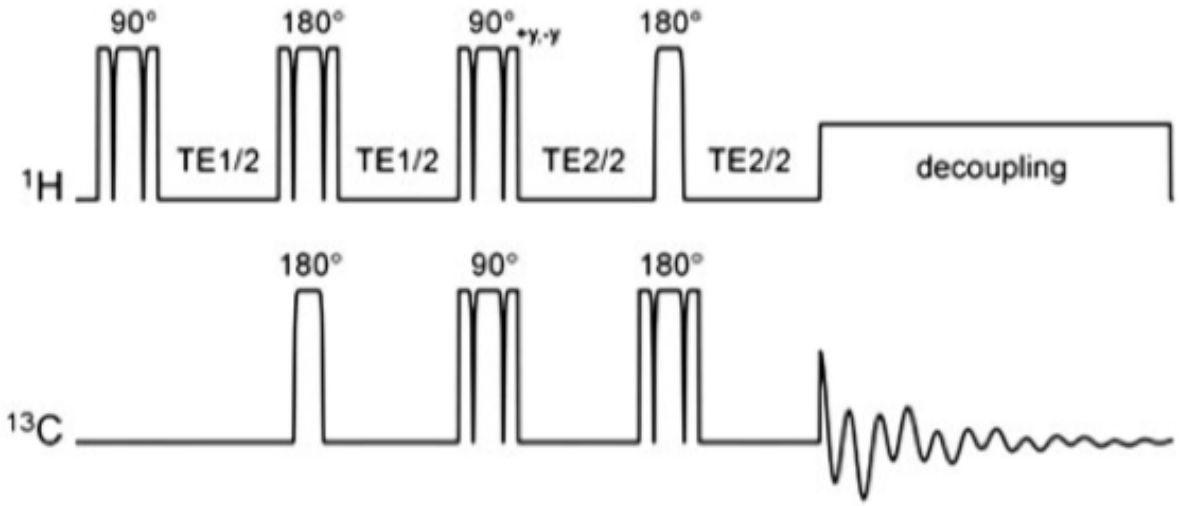

Figure 7. Polarization transfer sequence based on adiabatic AFP and BIR-4 pulses. The acquisition phase should be phase cycled in concert with the second ^{1}H 90° pulse to retain the transferred polarization and cancel direct ^{13}C magnetization. RF pulses are executed with BIR-4 waveforms, except for the first ^{13}C and last ^{1}H RF pulses, which are executed as shorter AFP pulses, thereby reducing RF power deposition. WALTZ-16 is often used for broadband decoupling during acquisition.

de Graaf, et al, NMR Biomed 2011

Methods: INEPT

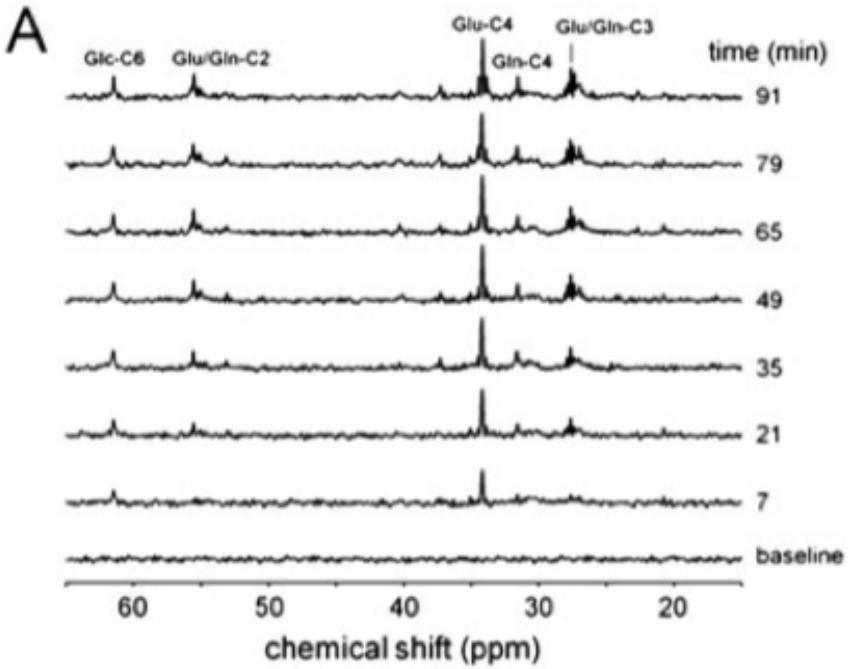

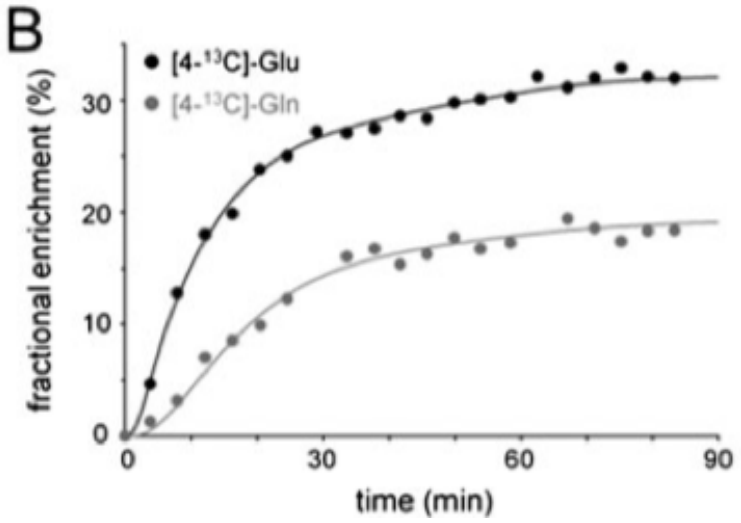

Human studies,
occipital lobe, 4T

de Graaf, et al, NMR Biomed 2011

A Key Result…

- Direct linkage between neuroenergetics and neurotransmitter flux
- 1:1 relationship between neuronal TCA and Glu/Gln cycling rates

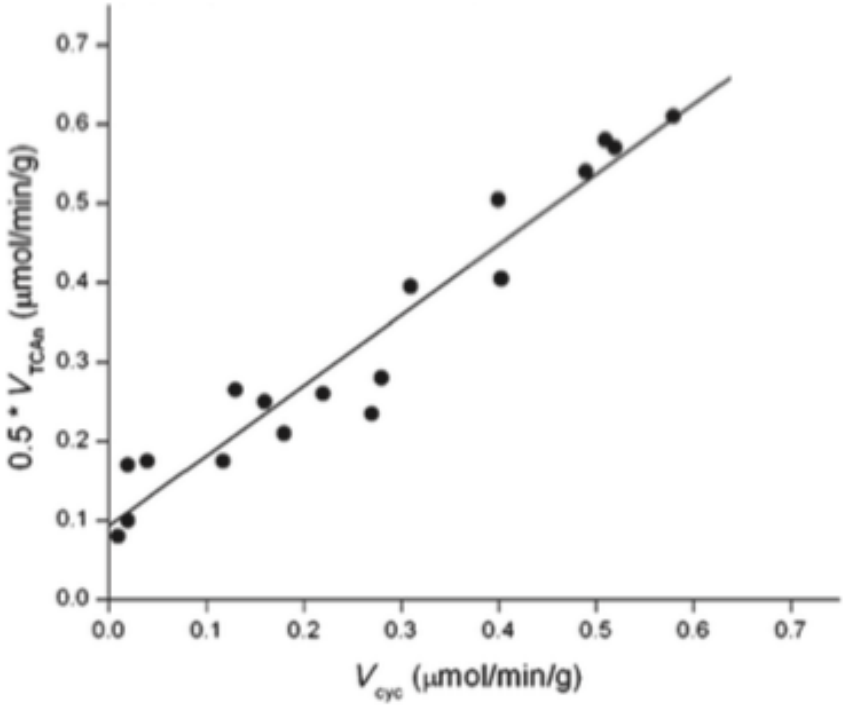

Rat cortex

Rothman, et al, NMR Biomed 2011

Methods: POCE

Proton-Observed Carbon Edited (POCE) LASER sequence

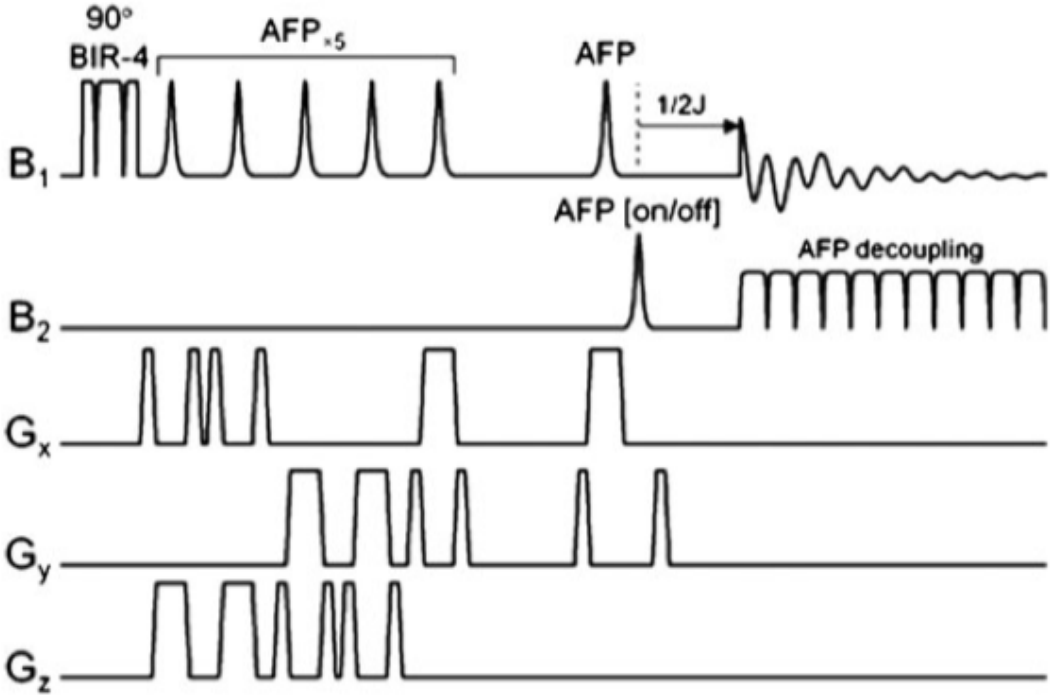

Rat brain, 9.4T, 90 min post
[1,6-^{13}C]Glc infusion

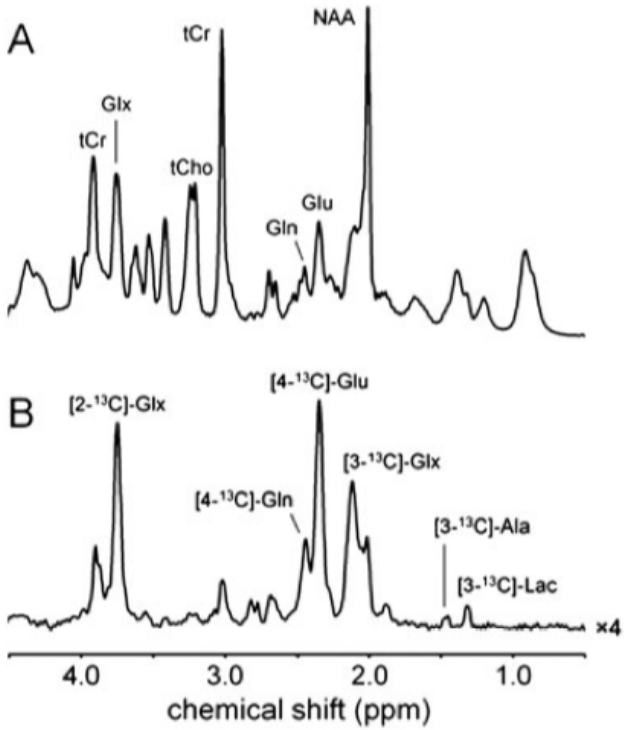

- Highest SNR: ^{1}H polarization + ^{1}H detection (16x over direct ^{13}C detection)
- However, requires high B0 (≥ 7T) due to small range of ^{1}H chemical shifts
- Requires SAR-intensive decoupling

de Graaf, et al, NMR Biomed 2011

Applications

- ^{13}C MRS provides the only nonivasive measurements of neurotransmitter cycling and cell-specific neuroenergetics.
- Major contributions to understanding…
  - Metabolic coupling between neurons and glia.
  - High neuronal activity of resting brain.
  - Alternations in neurological and psychiatric disease.
- Pathologies include: depression, drug addiction, epilepsy. metabolic disorders, hepatic encephalopathy, and neurodegenerative disorders.

Example: Aging

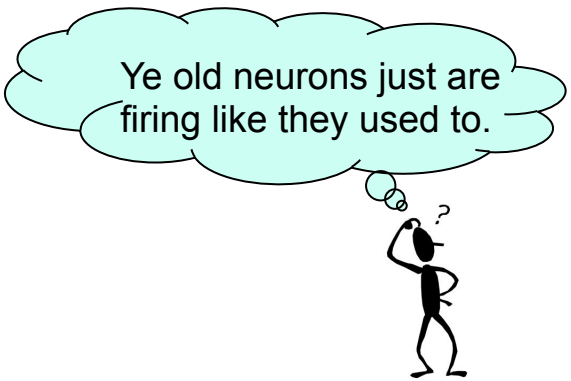

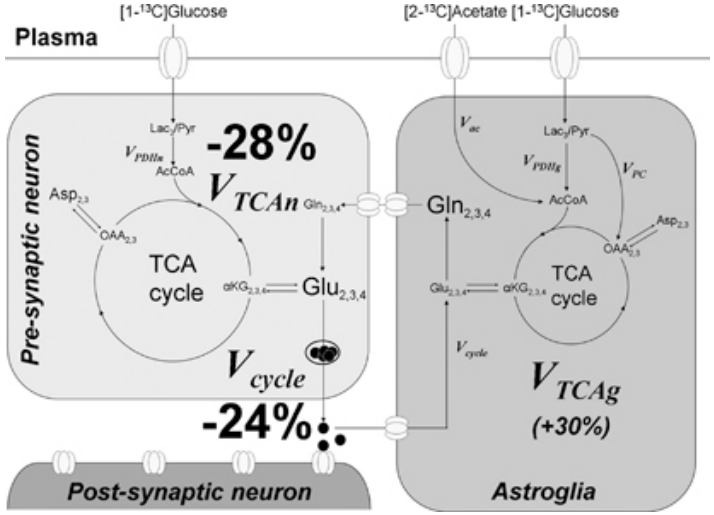

Boumezbeur, et al, Altered brain mitochondrial metabolism in healthy aging as assessed by in vivo magnetic resonance spectroscopy JCBFM, (2010) 30, 211–21

Open Research Questions

Improvements in the sensitivity and spatial resolution of ^{13}C MRS measurements

The primary limitation for the study of human brain disease by ^{13}C MRS is its low sensitivity, with the typical volume resolution being on the order of 25–100 cm^3. Substantial improvements have been achieved by detecting ^{13}C labeling indirectly via the *J* scalar coupling to bound protons (55,103), enhancing the spatial resolution to several cubic centimeters obtained at 4 T (57,84). However, because of the limited spectral resolution of ^{1}H MRS, only labeling of glutamate C4, the combined resonances of glutamate and glutamine C3, and lactate C3 have been reported, limiting the rates that can be measured to the neuronal TCA cycle or, in the case of elevated lactate, to glycolysis. With the advent of ultrahigh-field human MRS systems (7 T and above), in principle, it should be possible to measure resonances of glutamine and GABA, as has been demonstrated in animal studies (59,127,128), although the increased heating associated with decoupling at higher fields may limit this application.

Rothman, et al, NMR Biomed 2011

Current Methods

- ^{13}C MRS human brain studies are invariably performed in the occipital-parietal lobe.
- While most higher executive functions are performed in the frontal lobe, and neuropsychological disorders and cognitive deficits typically involve the frontal and temporal lobes, MRS requirements for **high-power decoupling** limit studies to the posterior brain.

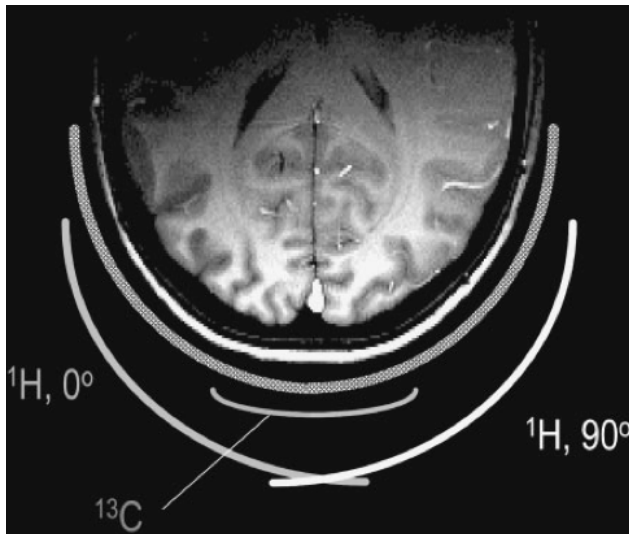

Problem Statement

- Decoupling directly bonded ^{13}C-^{1}H nuclei requires 180º echo-train spacing << 7ms
- Given a 200-300 ms readout (needed for spectral resolution), this translates to several hundred 180s spaced ~1ms apart = high-power decoupling!
- At 4T, decoupling SAR is just under the FDA limit for the back of the head.
- However, the lens of the eye, with little blood flow, has very poor heat dissipation, making high-power decoupling prohibitive.
- Hence, virtually all human ^{13}C MRS studies currently limited to the posterior brain.

Table 7 NRPB patient and volunteer SAR limits (Wkg^{-1}) for RF field exposure

NRPB level	Uncontrolled	Upper	Uncontrolled Peak SAR		
Body part	Whole*	Whole*	Head/ fetus**	Trunk**	Limbs**
Exposure time t < 15 min	2	4	4	8	12
Exposure time 15 > t < 30 min	30/t	60/t	60/t	120/t	180/t
Exposure time t >30 min	1	2	2	4	6

*Averaged over any 15-minute period. **Averaged over any 6-minute period.

How can we acquire ^{13}C MRS information from the anterior brain with sufficient quality to compute neuroenergetic and neurotransmitter cycling rates without eyeball cooking?

Decoupling

- MR method whereby the effects of J-coupling are removed.
- A series of 180º RF pulses on either of the coupled partners achieves the desired effect as long as the echo spacing $\tau << 1/J$.
- Decoupling is RF power intensive, thus minimum SAR is typically achieved using a low level continuous RF waveform (usually with phase modulation).

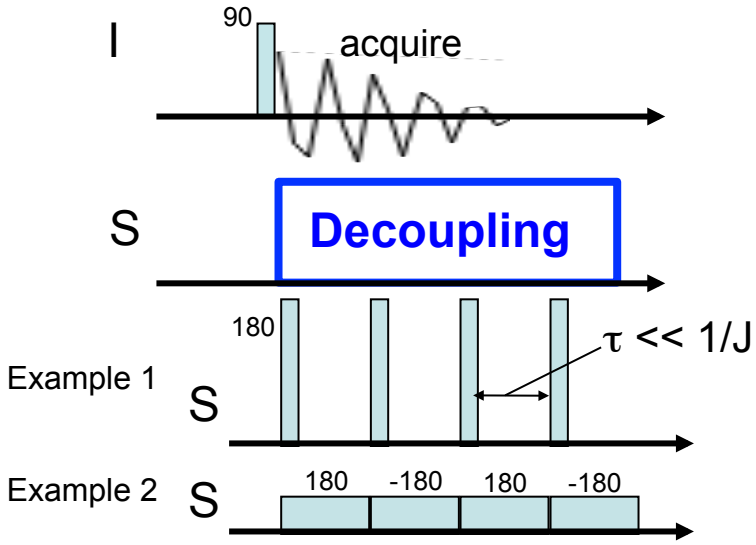

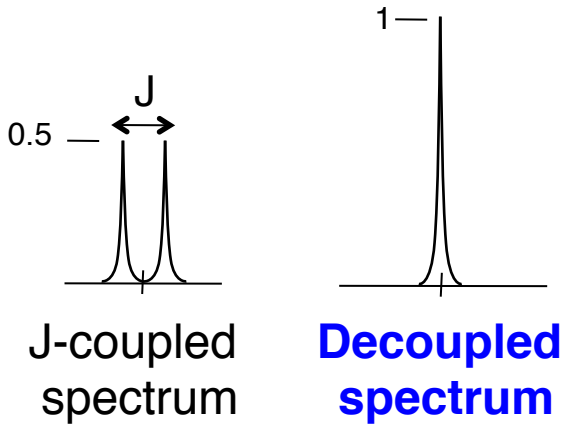

SAR depends on both τ and decoupling bandwidth

Importance of Decoupling

- Decoupling is very important for in vivo ^{13}C MRS studies, because J-coupling results in…
  - Loss of sensitivity
  - Overlapping peaks
- Example

[4-^{13}C]glutamate

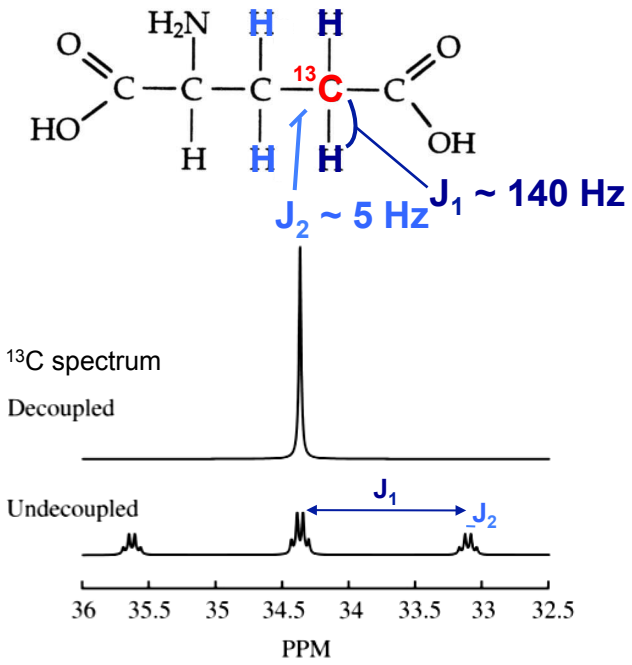

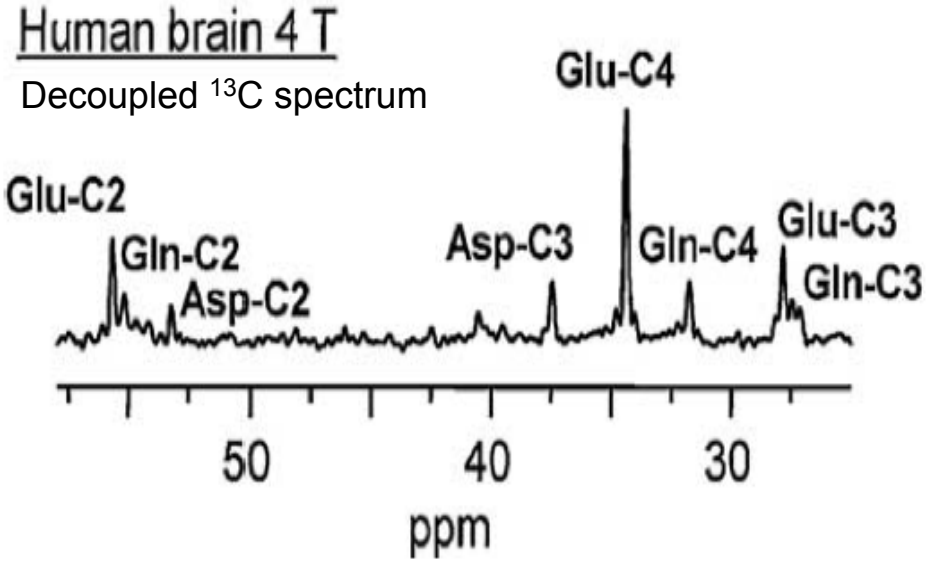

Note: $1/J_1 = 7$ ms

$1/J_2 = 200$ ms

Magnetization evolves in time…

- J-coupling looks like an additional “magnetic field”.

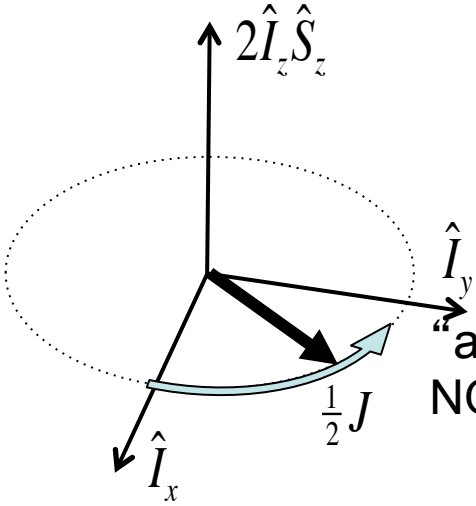

“anti-phase”–
NOT detected by coil.

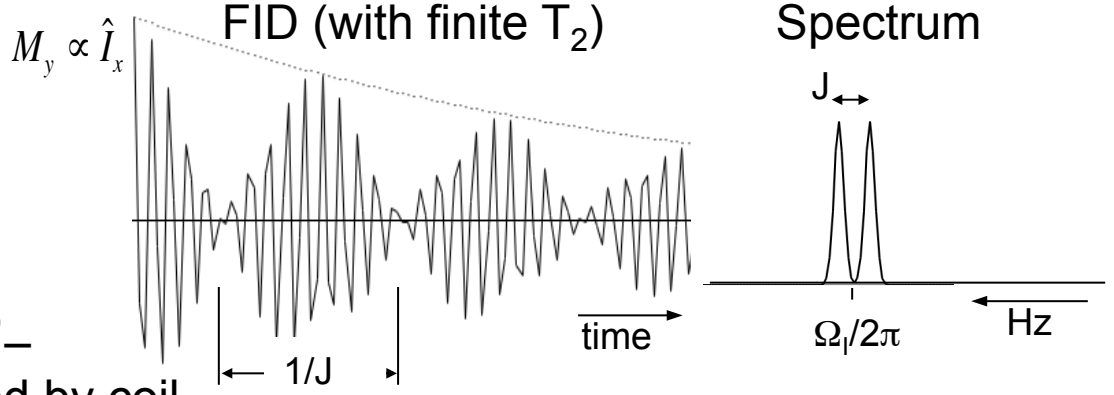

“in-phase”– Detected by coil.

In-phase
time evolution

$$\hat{I}_x \xrightarrow{\pi Jt} \begin{cases} \hat{I}_x \\ \hat{I}_y\hat{S}_z \end{cases}$$

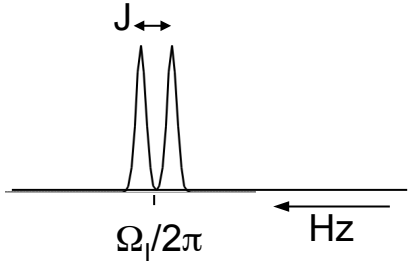

Anti-phase
time evolution

$$\hat{I}_x\hat{S}_z \xrightarrow{\pi Jt} \begin{cases} \hat{I}_x\hat{S}_z \\ \hat{I}_y \end{cases}$$

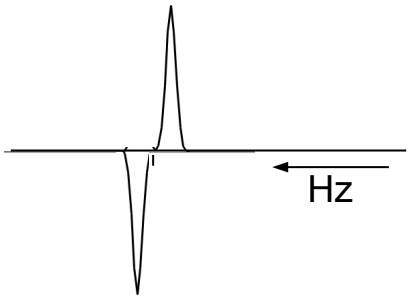

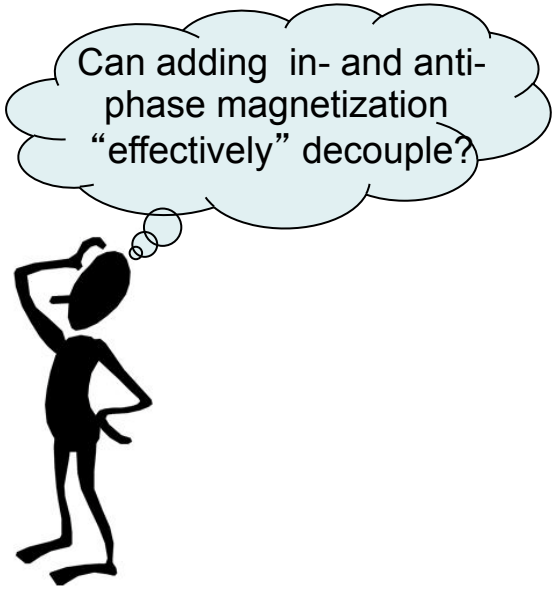

^{1}H-[^{13}C] Methods: PROCEED

PRoton Observed Carbon Edited Effectively Decoupled

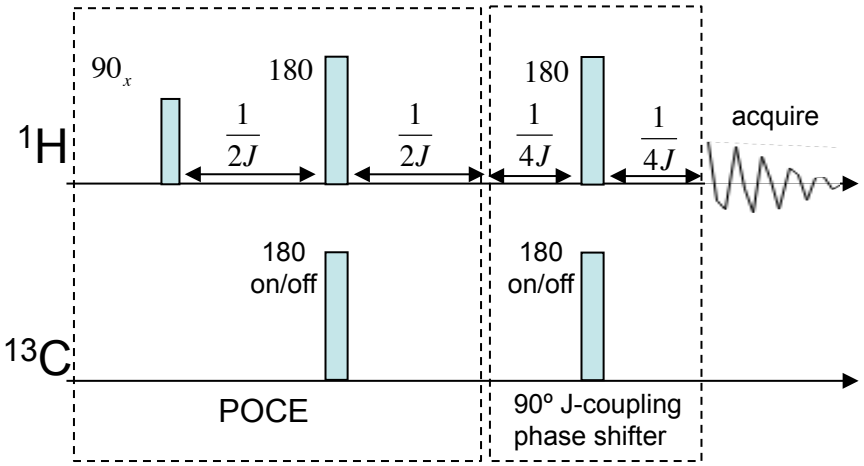

	Rf2 amplitude	Rf3 amplitude	Coherences
Acq 1	0	0	$\hat{R}_y + \hat{I}_y$
Acq 2	180	0	$\hat{R}_y - \hat{I}_y$
Acq 3	0	180	$\hat{R}_y - 2\hat{I}_x\hat{S}_z$
Acq 4	180	180	$\hat{R}_y + 2\hat{I}_x\hat{S}_z$
Recon: Acq 1 – Acq 2 ± *i* (Acq 4 – Acq 3)			

I = ^{1}H spins J coupled to ^{13}C, R = uncoupled ^{1}H spins

- PROCEED^{+} yields upfield peak
- PROCEED^{-} yields downfield peak.
- All ^{1}H chemical shifts refocused.
- Works for CH_n spin systems.
- Uncoupled spins suppressed.

[U-^{13}C]Glutamate

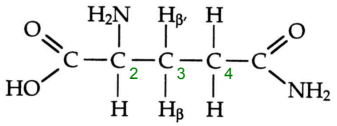

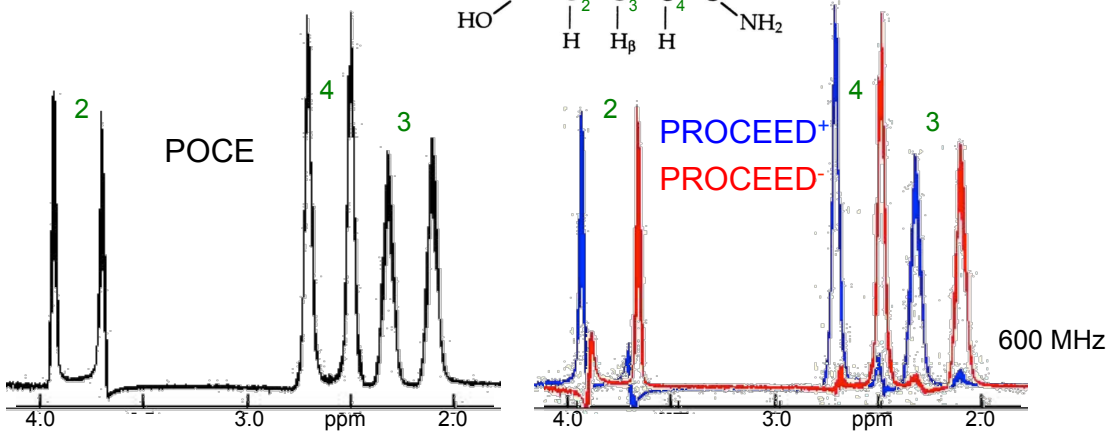

Heteronuclear Single Quantum Coherence (HSQC) MRS in Humans at 7 T

Robin A. de Graaf[1], Henk M. De Feyter[1], and Douglas L. Rothman[1]

[1]*MRRC, Yale University, New Haven, CT, United States*

ISMRM, 2015

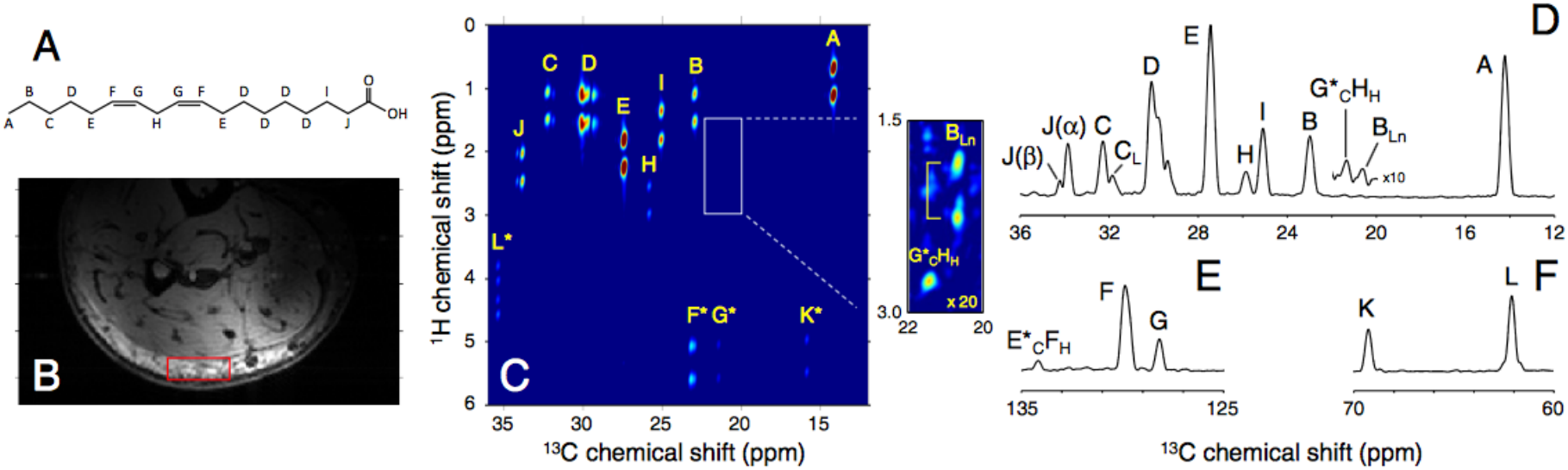

Figure 1: (A) Structure of linoleic acid which would be esterified to glycerol (carbons K and L) in a triglyceride. (B) Anatomical MRI of the leg showing the placement of a 3 x 1 x 3 cm voxel. (C) 2D HSQC spectrum acquired from human leg *in vivo* in 19 min with TR variation (TR1/TR2/T_1 = 3000/500/1000 ms). Labels with an asterisk (*) indicate that the resonance is aliased along the ^{13}C dimension by an integer number of the ^{13}C spectral width (= 2 kHz). The inset shows the linolenic acid resonance B_{Ln} with a 20-fold increased vertical scale, together with a ^{1}H-^{13}C resonance from correlation over multiple chemical bonds (HMBC) between the G position ^{13}C nucleus and the H position protons. (D) 1D projection of the ^{13}C fingerprint region summed over proton chemical shifts between 0.0 and 3.5 ppm. (E/F) 1D projection of the double-bond carbons (E) and glycerol carbons (F) summed over proton chemical shift ranges [4.5 . . . 6.0] ppm and [3.5 . . . 6.0] ppm (after appropriate ^{13}C frequency shifting), respectively.

RSNA 2014: PET-MR/Hyperpolarized MR Refresher Course

Hyperpolarized ^{13}C MR

A Complementary Method to PET for Imaging In Vivo Metabolism

Daniel M. Spielman, Ph.D.
Dept. of Radiology
Stanford University
Email: spielman@stanford.edu

Lucas Center for Medical Imaging

Dissolution Dynamic Nuclear Polarization

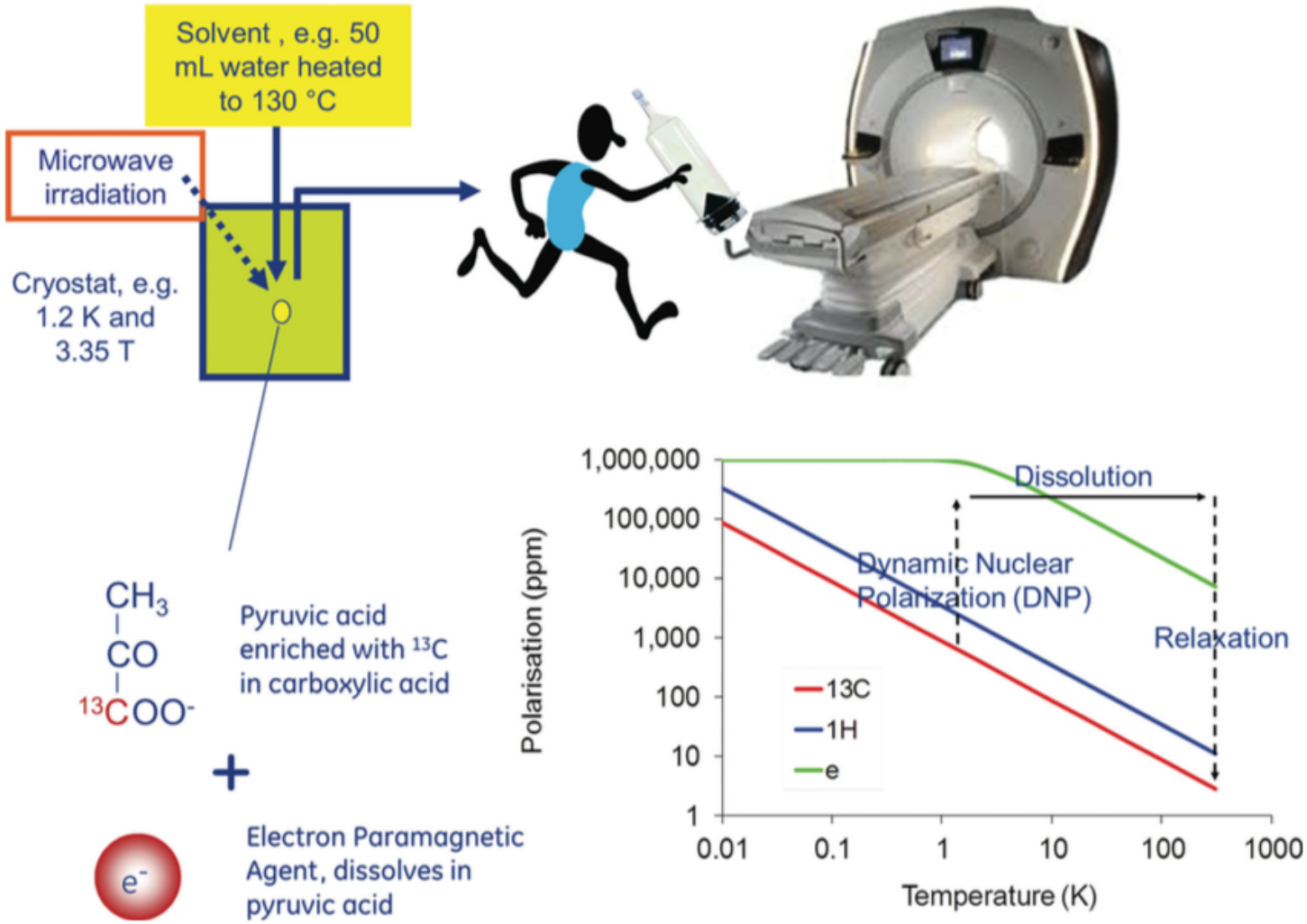

In Vivo Imaging Requirements

- Low toxicity (mM conc.)
- Long NMR relaxation times
- Chemical shift separation
- Rapid cellular uptake
- Rapid metabolism

Signal decays by relaxation and dilution

Polarization

T_1 decay

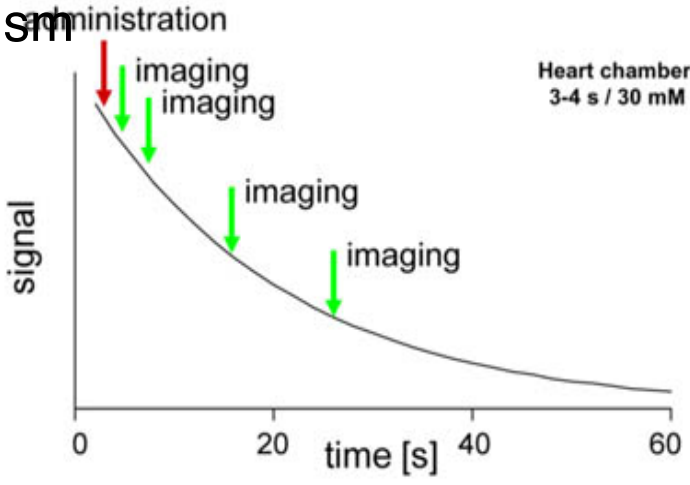

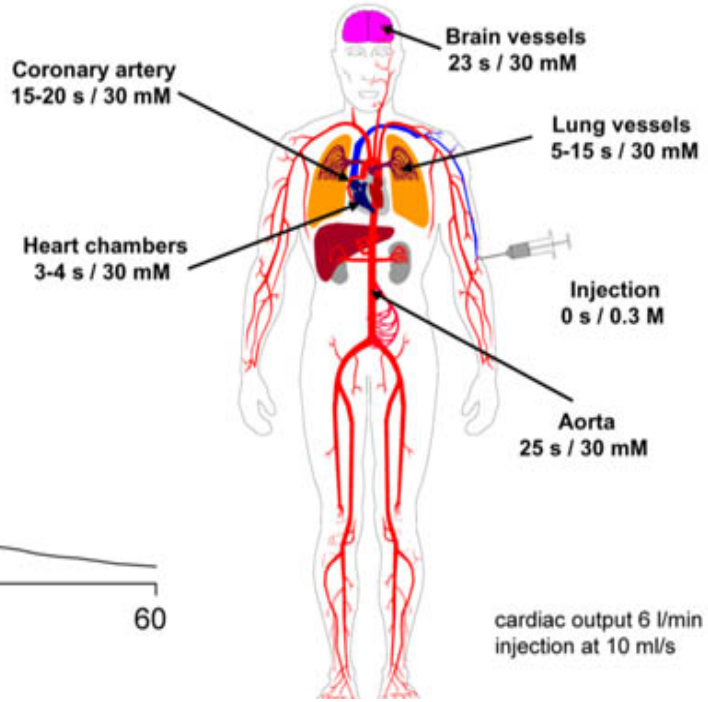

➡ Focus on low molecular weight endogenous compounds.

Example: [1-^{13}C]pyruvate

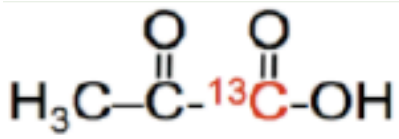

25% polarization ~ 30,000 fold signal gain!
In vivo T_1 = 30 s

Hyperpolarized [1-^{13}C]Pyruvate

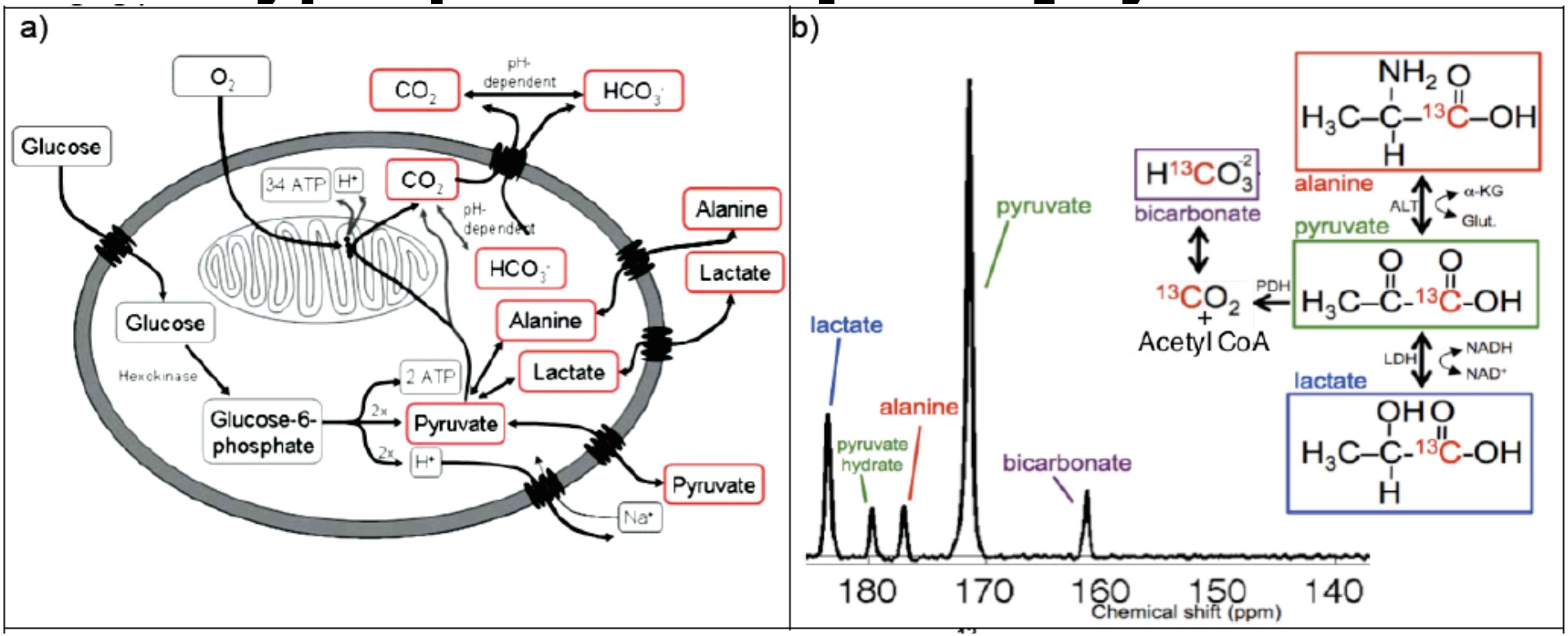

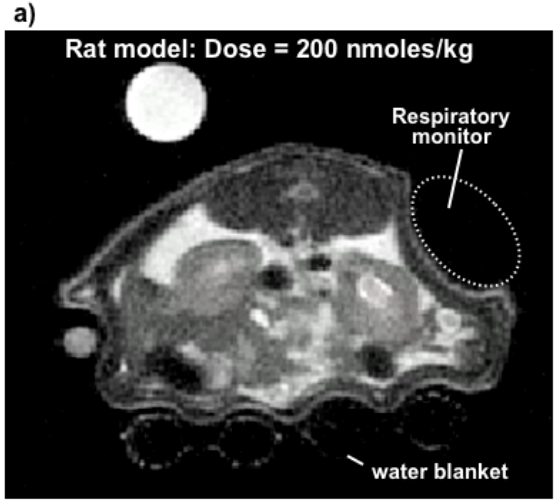

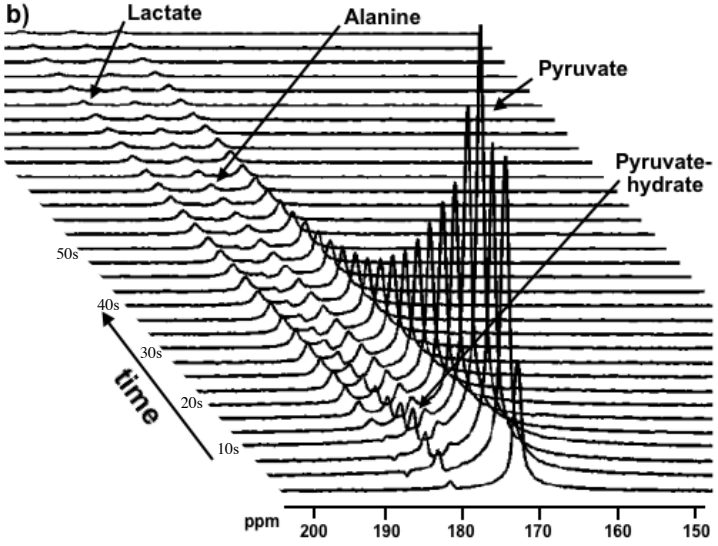

Time course of ^{13}C-MRS signals following the bolus injection of hyperpolarized ^{13}C-labeled pyruvate (samples taken every 3 s)

Cancer and the Warburg Effect

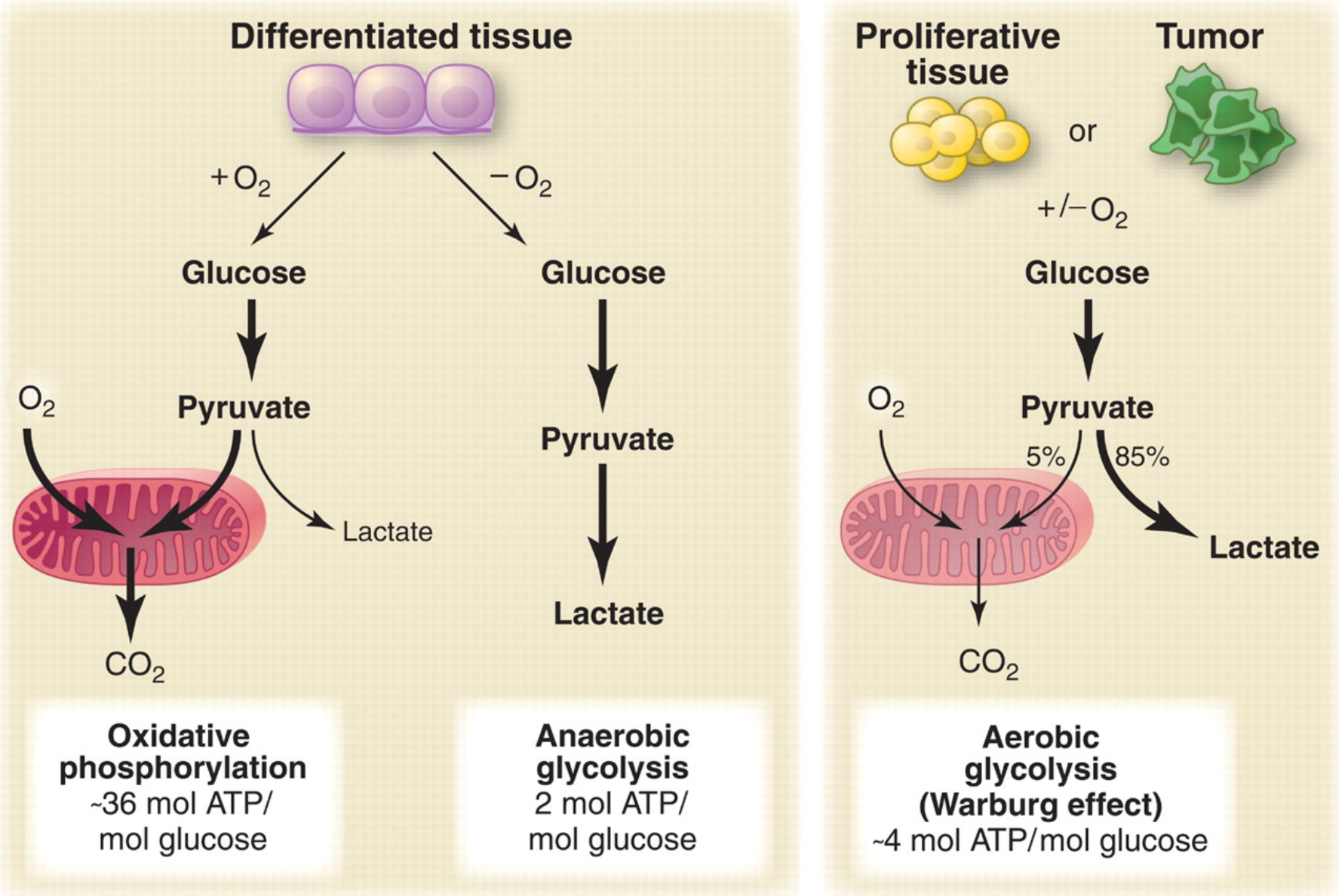

Cancer Res 2008; 68: (20). October 15, 2008 Research Article

Hyperpolarized ^{13}C Lactate, Pyruvate, and Alanine: Noninvasive Biomarkers for Prostate Cancer Detection and Grading

Mark J. Albers,[1,2] Robert Bok,[2] Albert P. Chen,[2] Charles H. Cunningham,[3] Matt L. Zierhut,[1,2] Vickie Yi Zhang,[2] Susan J. Kohler,[4] James Tropp,[5] Ralph E. Hurd,[5] Yi-Fen Yen,[5] Sarah J. Nelson,[1,2] Daniel B. Vigneron,[1,2] and John Kurhanewicz[1,2]

[1]Department of Bioengineering, University of California San Francisco and University of California Berkeley; [2]Department of Radiology and Biomedical Imaging, University of California San Francisco, San Francisco, California; [3]Sunny Brook Health Sciences Centre, Toronto, Ontario, Canada; [4]Union College, Schenectady, New York; and [5]GE Healthcare, Menlo Park, California

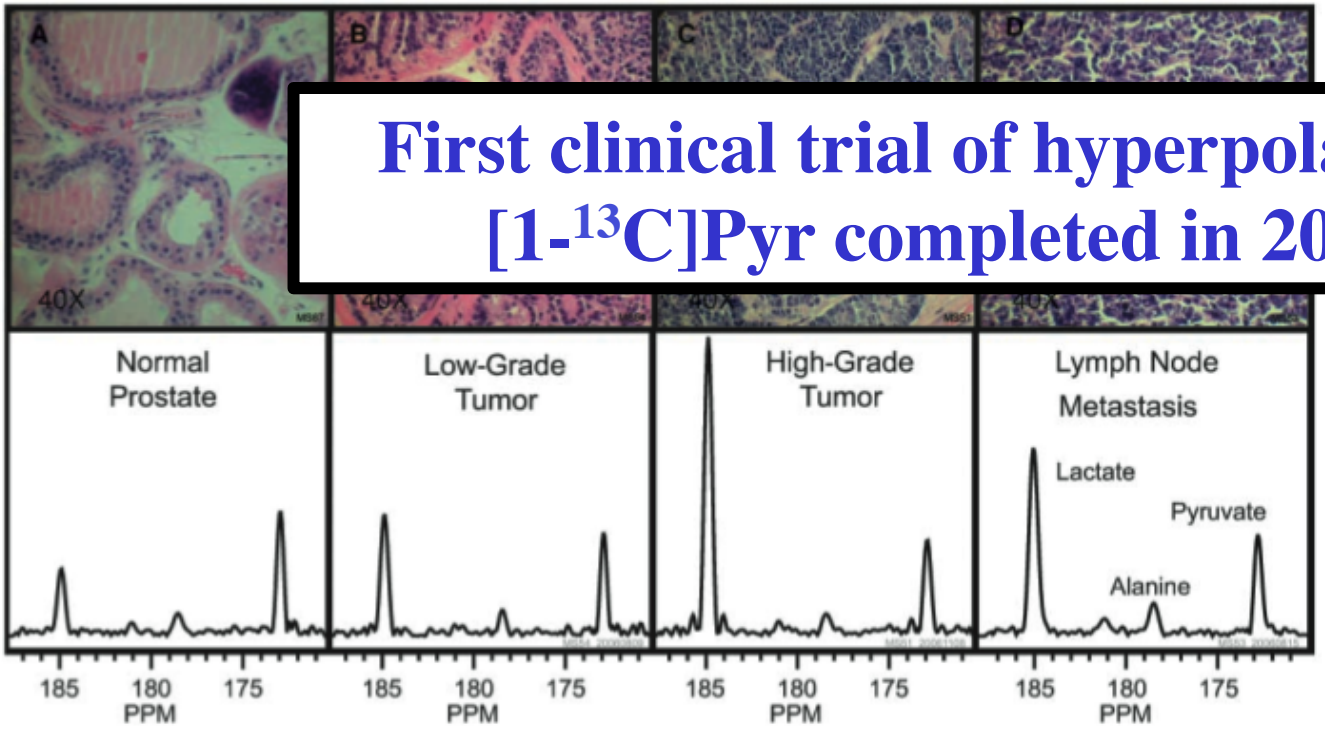

First clinical trial of hyperpolarized [1-^{13}C]Pyr completed in 2012.

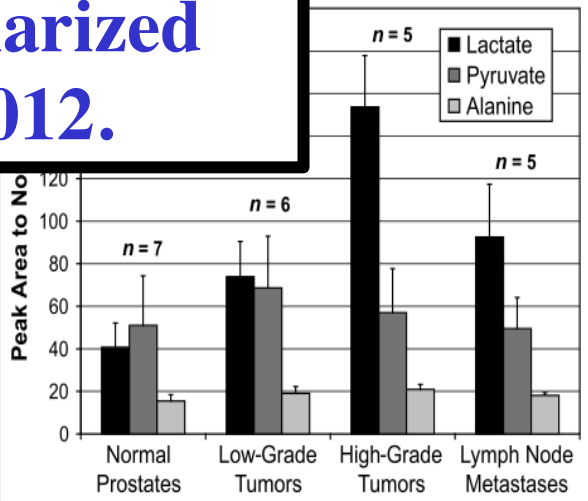

Magnetic Resonance in Medicine 59:1005–1013 (2008)

Cardiac Metabolism Measured Noninvasively by Hyperpolarized ^{13}C MRI

Klaes Golman,[1] J. Stefan Petersson,[1*] Peter Magnusson,[1] Edvin Johansson,[1] Per Åkeson,[2] Chun-Ming Chai,[3] Georg Hansson,[1] and Sven Månsson[3]

Pig Coronary Occlusion Model

Proton Perfusion Delayed enhancement Alanine Bicarb

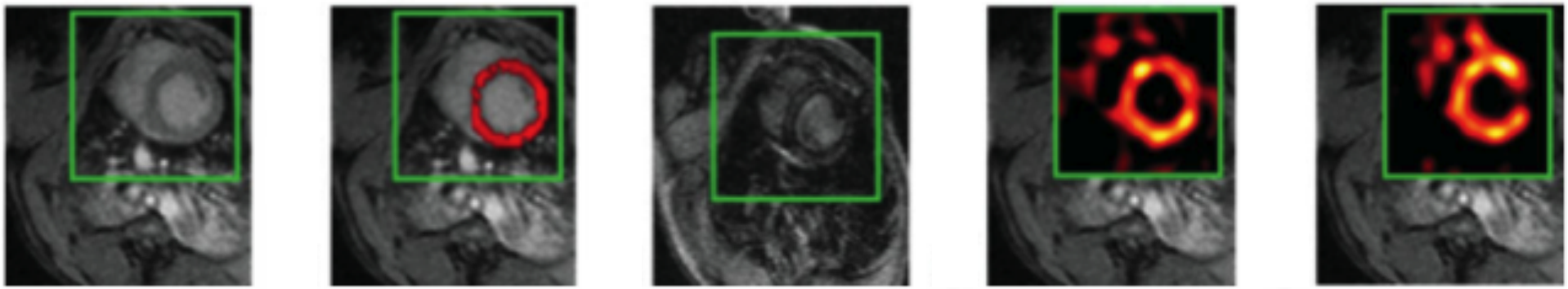

15 min occlusion (stunned) + 2 hrs reperfusion

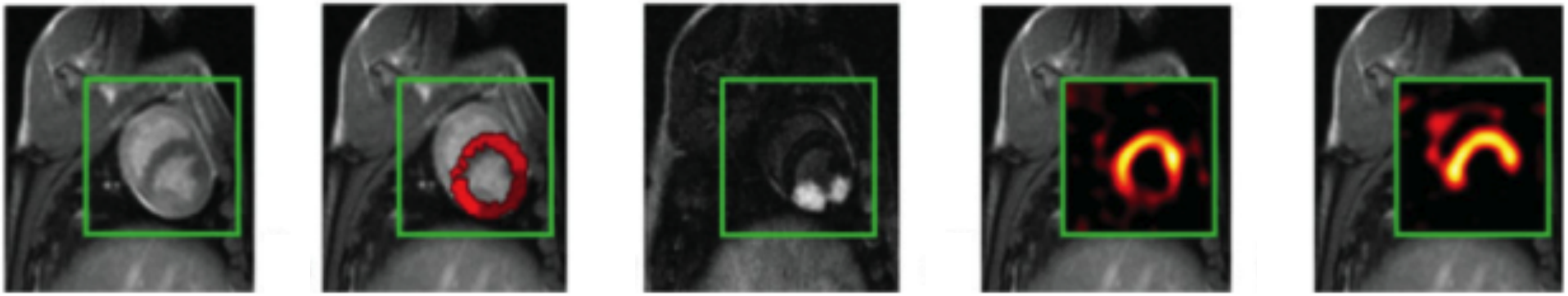

45 min occlusion (infarcted) + 2 hrs reperfusion

PNAS

Production of hyperpolarized [1,4-$^{13}C_2$]malate from [1,4-$^{13}C_2$]fumarate is a marker of cell necrosis and treatment response in tumors

Ferdia A. Gallagher[a,b,c], Mikko I. Kettunen[a,b], De-En Hu[a,b], Pernille R. Jensen[d], René in 't Zandt[d], Magnus Karlsson[d], Anna Gisselsson[d], Sarah K. Nelson[a,b], Timothy H. Witney[a,b], Sarah E. Bohndiek[a,b], Georg Hansson[d], Torben Peitersen[d], Mathilde H. Lerche[d], and Kevin M. Brindle[a,b,1]

[a]Cancer Research United Kingdom, Cambridge Research Institute, Li Ka Shing Centre, Robinson Way, Cambridge CB2 0RE, United Kingdom; [b]Department of Biochemistry, University of Cambridge, Tennis Court Road, Cambridge CB2 1GA, United Kingdom; [c]Department of Radiology, University of Cambridge, Addenbrooke's Hospital, Hills Road, Cambridge CB2 0QQ, United Kingdom; and [d]Imagnia AB, Box 8225, SE-200 41 Malmö, Sweden

Imaging necrosis

subcutaneous-implanted lymphoma

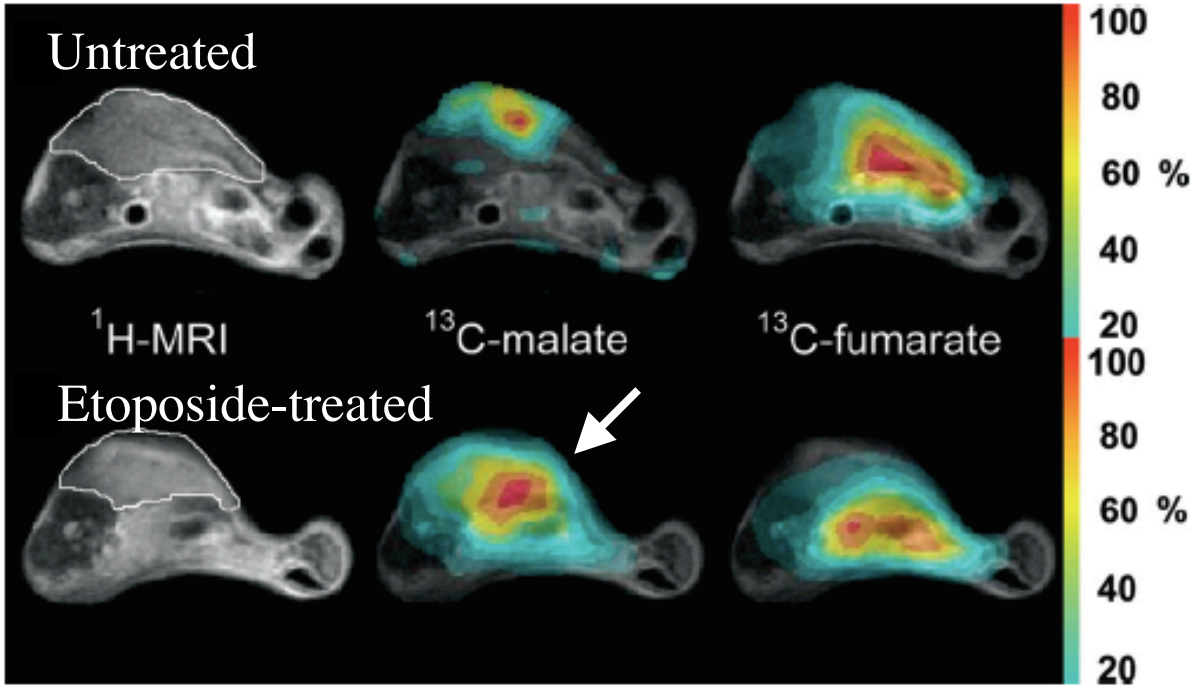

Journal of Nuclear Medicine, published on April 10, 2013 as doi:10.2967/jnumed.112.115402

Hyperpolarized [1-^{13}C]Dehydroascorbate MR Spectroscopy in a Murine Model of Prostate Cancer: Comparison with ^{18}F-FDG PET

Kayvan R. Keshari, Victor Sai, Zhen J. Wang, Henry F. VanBrocklin, John Kurhanewicz, and David M. Wilson

Department of Radiology and Biomedical Imaging, University of California San Francisco, San Francisco, California

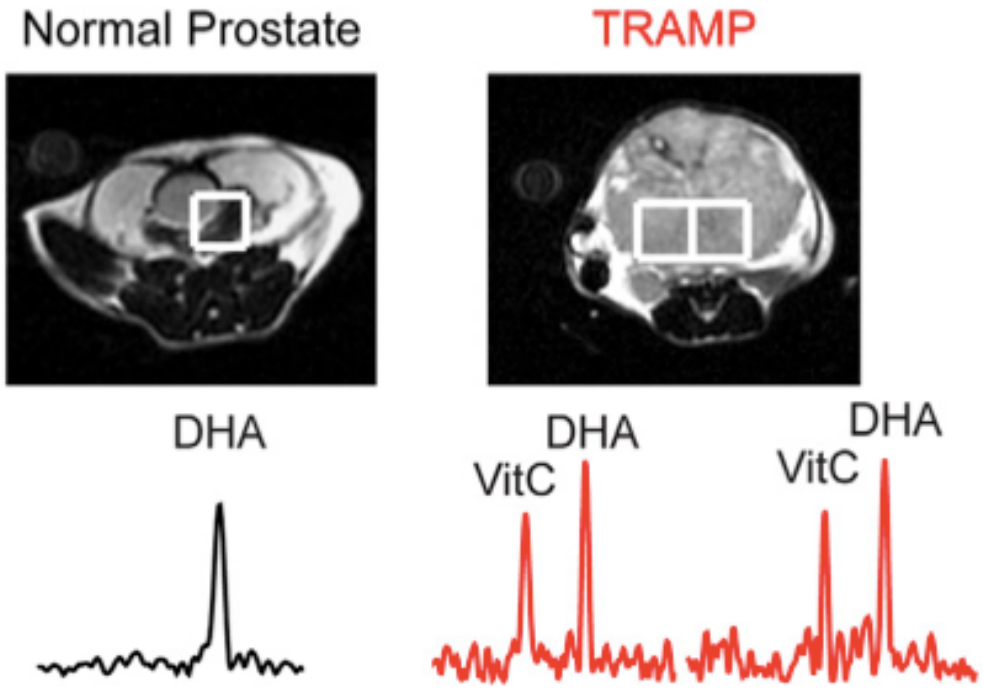

Imaging of redox or oxidative stress?

PET vs Hyperpolarized ^{13}C MRS

- Key idea: inject a "magnetically" enhanced biological substrate and image both the substrate and its downstream metabolic products.

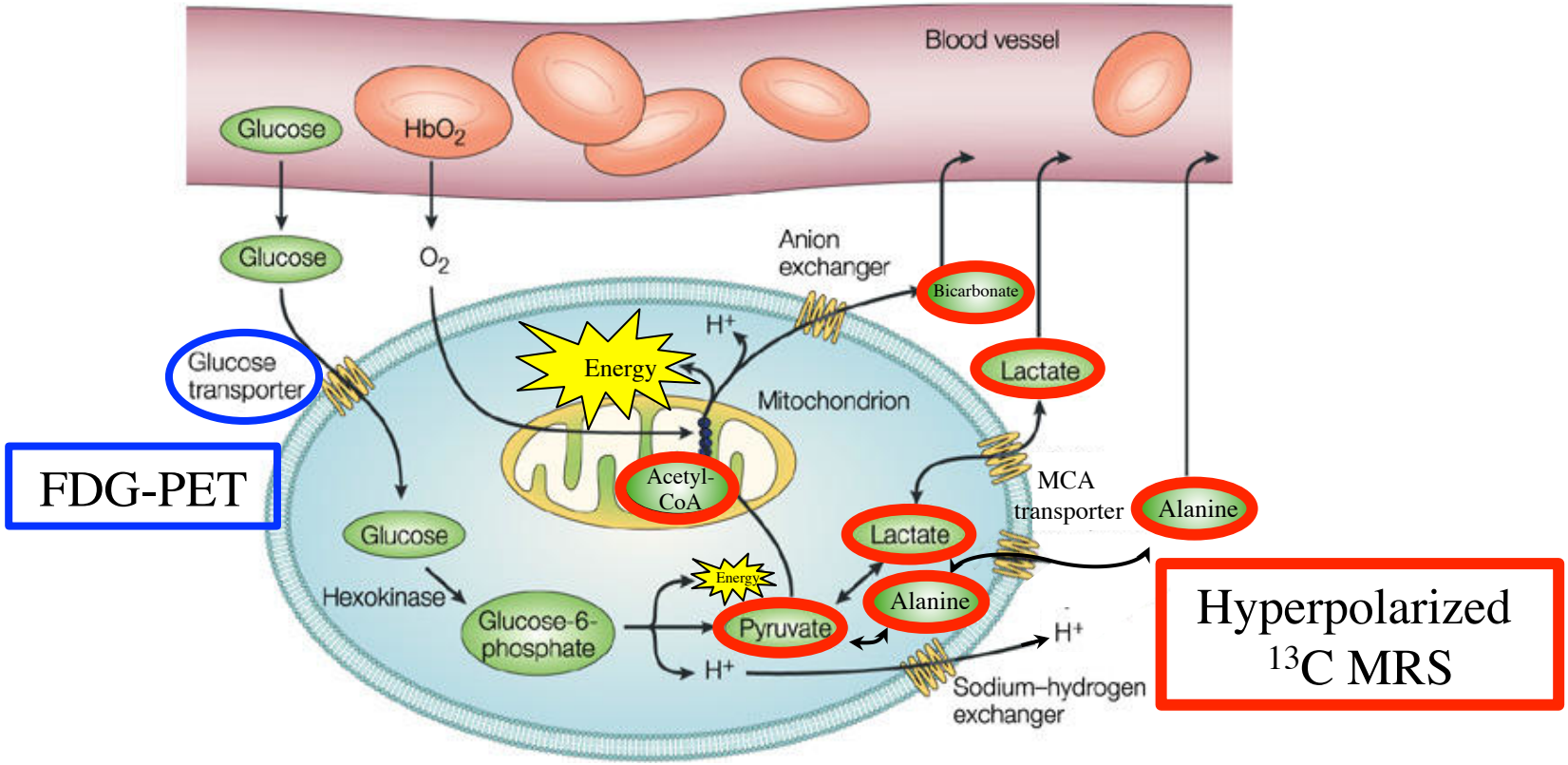

Am J Nucl Med Mol Imaging 2015;5(1):38-45

Original Article

Simultaneous hyperpolarized ^{13}C-pyruvate MRI and ^{18}F-FDG-PET in cancer (hyperPET): feasibility of a new imaging concept using a clinical PET/MRI scanner

Henrik Gutte[1,2*], Adam E Hansen[1*], Sarah T Henriksen[1,3], Helle H Johannesen[1], Jan Ardenkjaer-Larsen[3,4], Alexandre Vignaud[5], Anders E Hansen[2,6], Betina Børresen[7], Thomas L Klausen[1], Anne-Mette N Wittekind[1], Nic Gillings[1], Annemarie T Kristensen[7], Andreas Clemmensen[1,2], Liselotte Højgaard[1], Andreas Kjær[1,2]

Received September 14, 2014; Accepted September 29, 2014; Epub December 15, 2014; Published January 1, 2015

Abstract: In this paper we demonstrate, for the first time, the feasibility of a new imaging concept - combined hyperpolarized ^{13}C-pyruvate magnetic resonance spectroscopic imaging (MRSI) and ^{18}F-FDG-PET imaging…We propose that this new concept of simultaneous hyperpolarized ^{13}C-pyruvate MRSI and PET may be highly valuable for image-based non-invasive phenotyping of tumors…treatment planning and therapy monitoring.

Canine Liposarcoma

Am J Nucl Med Mol Imaging 2015;5(1):38-45

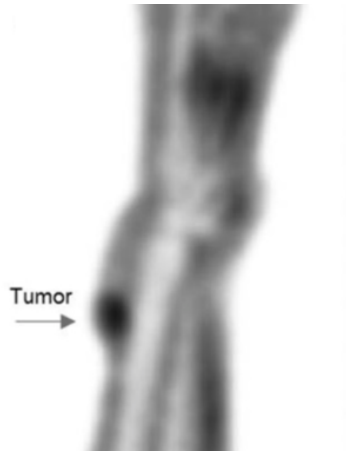

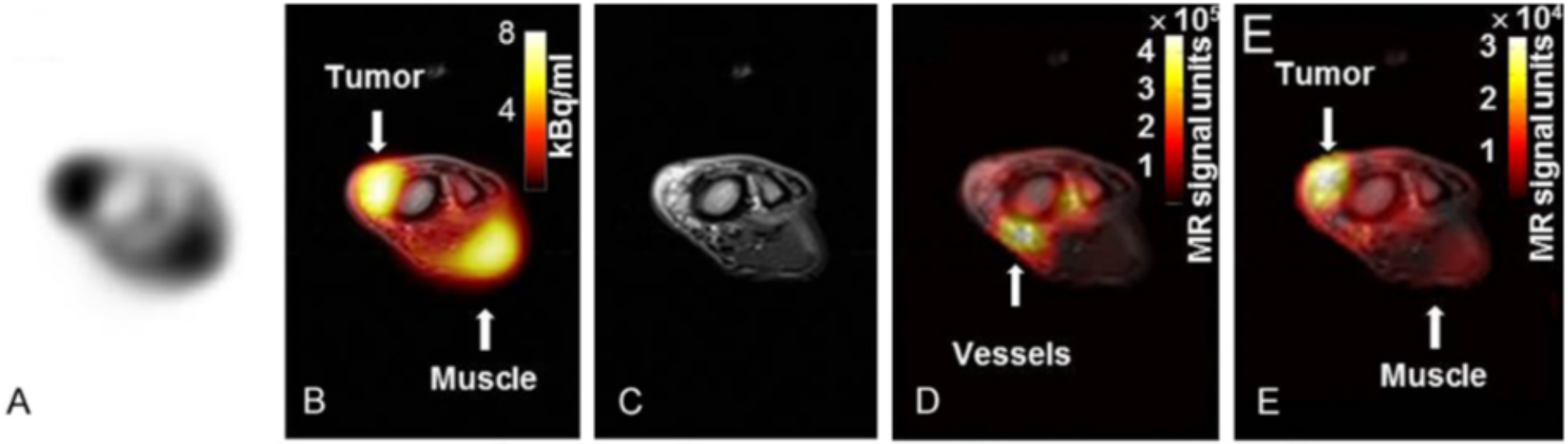

PET/MR/^{13}C Center for Metabolic Imaging

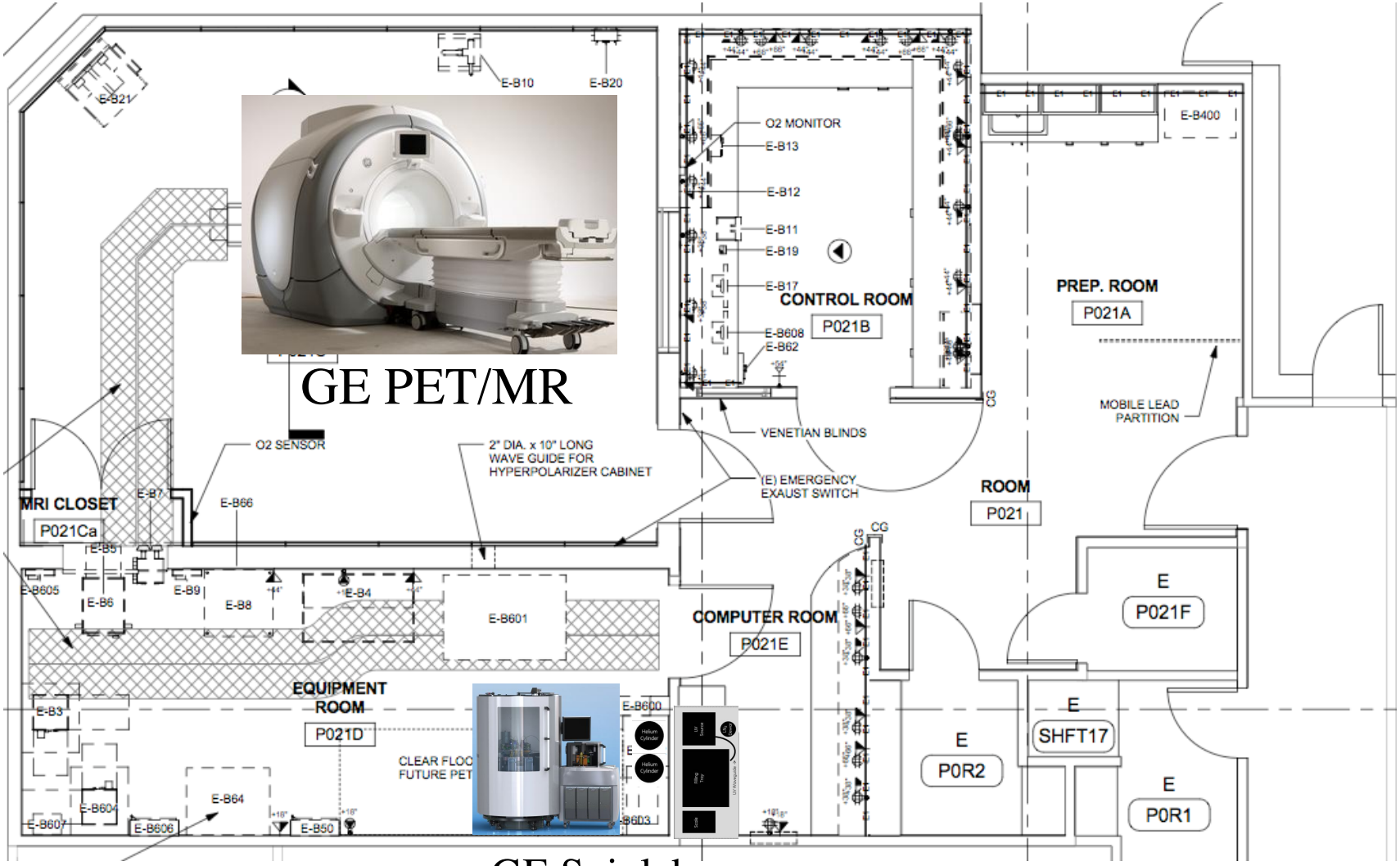

GE PET/MR

GE Spinlab

The End.

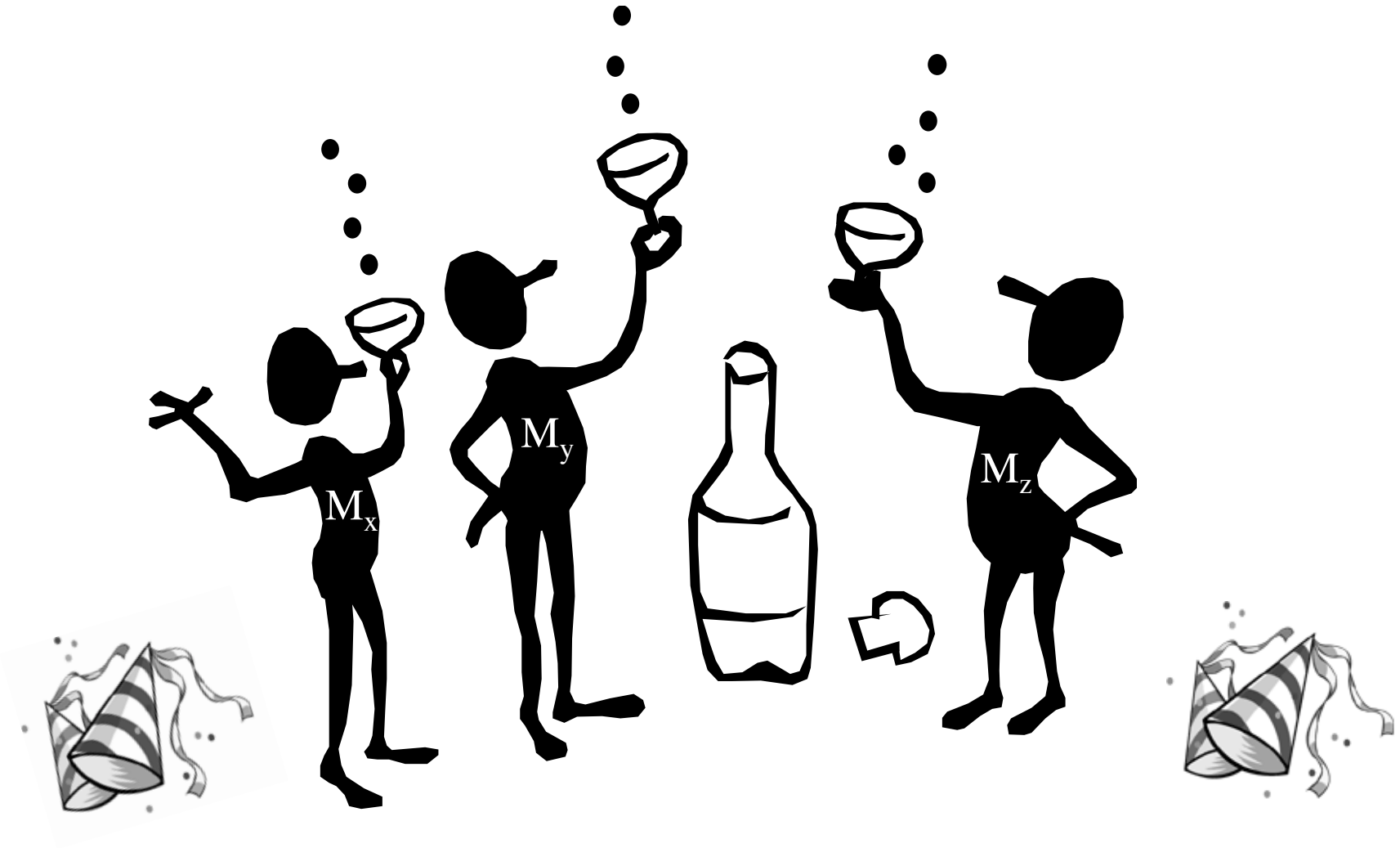

(Please fill out the course evaluations forms!)